Results in Engineering 29 (2026) 108415

Contents lists available at ScienceDirect

Results in Engineering

journal homepage: www.sciencedirect.com/journal/results-in-engineering

Enhancing sulphate and sulphuric acid resistance of low-carbon concrete using waste ceramic tiles and silica nanoparticles synthesized from recycled bottle glass

Zahraa Hussein Joudah [a], Nur Hafizah A. Khalid [b,*], Mohammad Hajmohammadian Baghban [c,*], Iman Faridmehr [d,e], Masoumeh Khamehchi [e], Ghasan Fahim Huseien [e,f,*]

[a] Department of Civil Engineering, Faculty of Engineering, University of Misan, Amarah 62001, Iraq
[b] Faculty of Civil Engineering, Universiti Teknologi Malaysia, Johor Bahru, Johor 81310, Malaysia
[c] Department of Manufacturing and Civil Engineering, Norwegian University of Science and Technology (NTNU), Gjøvik 2815, Norway
[d] Civil Engineering Department, Faculty of Engineering, Girne American University, N. Cyprus Via Mersin 10, Turkey
[e] EcoStruct Building Technologies B.V., Fluwelen Burgwal 58, The Hague 32511 CJ, the Netherlands
[f] Department of the Built Environment, School of Design and Environment, National University of Singapore, 117566, Singapore

ARTICLE INFO

Keywords:
Nanoparticles
Wastes tile ceramic
Modified concrete
Sulphuric acid
Sulphate resistance
Low-carbon constuction materials

ABSTRACT

Concrete has low performance in sulfuric acid environment because of its alkaline nature and shown very high degree of deterioration after exposure period. In recent years, the development of long-lasting cement binders has become a key priority in the construction industry. This study involved to develop high resistance concrete to sulphuric acid attacks utilizing industrial wastes such as tile ceramic and bottle glass. Concrete specimens were prepared with fully crushed ceramic as natural aggregate replacement, the ordinary Portland cement (OPC) was replaced with 60 % of wastes tile ceramic powder (WTCPs) incorporating varying level (2 %, 4 %, 6 %, 8 % and 10 %) of silica nanoparticles from wastes bottle glass. The performance of the designed concrete was assessed after 6 and 12 months of exposure to a 10 % suphuric acid and sulphate solutions using several tests, including residual compressive strength, weight loss, ultrasonic pulse velocity (UPV), visual inspection, and microstructural analysis. The experimental findings revealed a notable enhancement in the durability of the proposed concrete against sulphuric acid and sulphate attacks when 60 % of OPC was replaced with WTCPs combined with 4–6 % waste bottle glass nanoparticles (WBGNPs). After 12 months of exposure to sulfuric acid, incorporating WTCPs and WBGNP into the cement matrix significantly reduced strength, weight, and UPV losses from 74.3 %, 15.4 %, and 66.9 % to 37.9 %, 8.1 %, and 34 %, respectively. A similar trend was observed under sulphate attack, where losses decreased from 15.1 %, 3.3 %, and 31.5 % to 1.4 %, 1.7 %, and 7.3 %. The substitution of cement with WTCPs and WBGNPs enhances concrete durability by refining pore structure and lowering permeability. The pozzolanic reaction between aluminosilicate and calcium hydroxide generates additional calcium silicate hydrate (C–S–H) gel, which densifies the matrix, limits microcrack formation, and strengthens resistance to chemical ingress. Consequently, this process effectively controls the excessive formation of gypsum and ettringite, reducing deterioration, extending service life, and improving overall performance in aggressive environments. Its concluded that using high volume of WTCPs incorporating silica nanoparticles leads to produce high performance concrete to aggressive environments with many environmental benefits such as minimize the demand of natural resources, reduce the landfill problems and contribute to control the carbon dioxide emission by reduce the used cement in construction industry.

* Corresponding authors.
E-mail addresses: nur_hafizah@utm.my (N.H.A. Khalid), mohammad.baghban@ntnu.no (M.H. Baghban), eng.gassan@yahoo.com (G.F. Huseien).

https://doi.org/10.1016/j.rineng.2025.108415
Received 19 August 2025; Received in revised form 16 November 2025; Accepted 22 November 2025
Available online 24 November 2025

1. Introduction

In construction industry, concrete is widely used and researched due to its availability of local materials, low cost, adaptable composition, and ease of construction [1,2]. Concrete plays a critical role in infrastructure development but is associated with significant environmental impacts due to the high carbon emissions from ordinary Portland cement (OPC) production [3,4]. However, with increasing the demand of cement in construction industry, the carbon dioxide emission from this industry trend to increase and contributed to 8 % of total greenhouse emission [5–7]. Several technologies have been adopted to reduce CO_2 emissions from cement production, including material efficiency strategies (such as optimizing mix design and extending service life), the use of alternative materials, fuel switching, energy-efficiency improvements, and carbon capture and storage [8–10]. The use of alternative materials—particularly supplementary cementitious materials (SCMs) as partial replacements for cement—is widely practiced. Various types of low-carbon cement are now produced using industrial by-products such as fly ash, slag, and rice husk ash, etc. Incorporating SCMs into the cement matrix not only reduces CO_2 emissions but also improves the mechanical performance and extends the service life of concrete by enhancing its durability in aggressive environments. Concrete durability generally increases with higher SCM content; however, the compressive strength often declines when SCMs exceed approximately 20–30 % [11,12]. This presents a major challenge for producing ultra-durable, low-carbon concrete using high SCM volumes (up to 50 % cement replacement).

Ordinary Portland cement concrete is generally known for its low resistance to sulfuric acid exposure. It is widely accepted that concrete structures show reduced durability in aggressive environments, including sulfuric acid and sulphate conditions, which can greatly shorten their service life [13]. In a study by Metha [14] related to concrete's durability and progress for next half century they identified the primary reasons for the failure of concrete in terms of it hierarchy order including corrosion of steel, frost-mediated damages in the cold climate, and physicochemical reaction under the exposure of corrosive environment. The pH values of concrete typically range between 11 and 12. When exposed to acidic substances, concrete undergoes a redox reaction that breaks the calcium hydroxide and various products emerge from cement hydrations, weakening its strength and durability [15]. Notably, H_2SO_4 is a major harmful chemical agent that affects concrete, causing both acid and sulphate corrosion. In engineering practice, sulphuric acid environments are commonly encountered, such as in acid rain [16–18], industrial settings, and sewage treatment systems [2,19,20]. Consequently, research on concrete's resistance to sulphuric acid has gained increasing attention, with scholars conducting various studies. However, there is currently no standardized method for evaluating concrete's resistance to sulphuric acid [21,22]. To assess the damages of concrete, most researchers rely on various easily measurable indicators like visual appearance, corrosion depth, mass loss, and strength loss after subjected to H_2SO_4 solution for specific durations. Surface roughness is also a key factor influencing the bonding performance between concrete and rock interfaces [23], and the surface of contact amid casted concrete and precast.

Although it can tolerate brief contact with mild acids, OPC cannot withstand solutions with a pH of 3 or below[24]. Sulfuric acid is especially damaging to concrete because it causes both acid attack and sulfate attack. The degradation of concrete sewer pipes due to sulfuric acid is a widespread global issue. Additionally, industrial waste often contains significant amounts of sulfuric acid, exposing concrete structures in industrial areas to potential damage. Sulfuric acid reacts with calcium hydroxide, a cement hydration product in concrete, forming expansive gypsum and ettringite [25,26]. The formation of gypsum in concrete results in increased volume, leading to internal stress, expansion, and micro-cracks [12]. Gypsum interacts with calcium aluminate hydrate (C_3A), leading to the formation of ettringite, which has a volume nearly seven times greater than the original compound [27]. The presence of ettringite generates internal pressure within the concrete, causing cracks [20]. Over time, the corroded concrete loses its mechanical strength, which leads to further cracking, spalling, and eventual destruction [28].

A global rise in concrete structure damage due to acid exposure has become noticeable. This is mainly driven by the growing presence of acidic environments resulting from expanding urban and industrial activities [29]. Acidic conditions can also originate from agricultural sources. Given the high susceptibility of cementitious materials to acid exposure, the study of acid attacks on concrete is of significant importance [30–32]. Many researchers have examined the durability of cement materials when exposed to various acids, particularly solutions with a pH lower than, equal to, or higher than 4 [33]. Several studies have concentrated on the impact of strong acids, including sulfuric acid (H_2SO_4), hydrochloric acid (HCl), carbonic acid (H_2CO_3), and phosphoric acid (H_3PO_4) [8], on cement materials, mortar, and concrete without mineral additives [34].

The hydration bond of concrete is weakened under the exposure of sulphuric acid, resulting in substantial damage and durability reduction [35,36]. Nonetheless, the concrete must possess sufficient strength to extend the lifespan of construction projects, withstand weathering-related issues, attack by chemicals, abrasions, and other types of deteriorations, while upholding its anticipated performance [37]. Traditional concrete is vulnerable to chemicals attack especially to acid and sulphates, raising considerable distress. Studies showed that OPC-based concrete's alkaline nature make them prone to acids attack, causing the cement paste components to disintegrate upon exposure to acids [38].

Acid degradation of concrete structures present substantial challenges for strength and durability performance related to the facilities of bio-gases and water treatments [39,40]. Sulfuric acid attack, in particular, is a common cause of damage to concrete's durability. The reactions amid the surface particles on concrete can lead to the formation of ettringite, gypsum, and other corrosive by-products [41]. Upon contact with sulfuric acid, concrete begins to deteriorate, and this deterioration can be categorized into two stages. The first stage involves the interaction with calcium hydroxide, while the second stage results from the reaction with calcium silicate hydrate [42]. These chemical processes cause changes in the weight, strength, and microstructure of both concrete and mortar, affecting their physical and chemical properties. Such factors must be carefully considered during construction, particularly in coastal regions [43]. Therefore, the issue of sulfuric acid attack is a key area of research in structural engineering, drawing significant attention worldwide [44].

The influences of H_2SO_4 on the properties of concrete have widely been studied. The effect of high volume of aluminosilicate wastes inclusion in concrete as a SCM for partial replacement of OPC was examined [45]. Their findings indicated that adding this material enhanced the concrete's resistance to acid. The authors concluded that the inclusion of these materials improved the concrete's resistance to acid. Additionally, Chindaprasirt et al. [46] found that H_2SO_4 leads to the OPC-based concrete's weight losses that increase with exposure time in acid. The impact of substituting up to 20 % of OPC weight with sugarcane bagasse ash in cement paste and mortar was examined, revealing a significant enhancement in the concrete's resistance to sulfuric acid attacks, thereby reducing both strength and weight loss percentages [47]. It was suggested [48] that 21 % replacement of OPC with SCMs can enhance the durability performance, as SCMs preserve the reference cement's key characteristics. In another investigation [49], the authors reported that the inclusion silica fume (SF) leads to reduce the weight loss after exposure to 3 % H_2SO_4 solution and enhanced it durability performance and residual strength. Joshaghani and Moeini [50] by incorporating rice husk ash and bagasse, wherein the inclusion of these materials was found to enhance the acid resistance mortars.

Nanosilica serves as an efficient binder for cement and aggregates due to its large specific surface area [51], and small particle size, which

contribute to its high pozzolanic activity [52]. However, because of their high reactivity and mobility, silica nanoparticles used in the concrete industry present notable environmental risks. Mitigating these risks requires the implementation of engineering controls, proper handling procedures, personal protective measures, and comprehensive training. By reducing permeability, nanosilica particles effectively fill voids and pores [53], thereby strengthening the Interfacial Transition Zone (ITZ). Additionally, nanosilica accelerates the concrete hydration process, promoting the formation of calcium-silicate-hydrate (C-S-H) gel [52], which further enhances the overall strength of the concrete [53]. When a reaction between nanosilica and $Ca(OH)_2$ takes place, the Portlandite ($Ca(OH)_2$) content goes down, forming a dense material [54]. In terms of resistance to corrosion and extreme temperatures, mechanical properties and durability are enhanced when nanosilica is added to cement at 4 % [55–57]. Poor dispersion can produce agglomeration [55,57] and reduce workability [56] when high amount of nanosilica is used, and nanosilica replacement is best performing at 0.5–4 %.Therefore, using nano-silica together with a high volume of supplementary cementitious materials as a cement replacement can provide an effective solution to improve the low strength performance of proposed concrete.

The use of Artificial Intelligence (AI) in the construction sector, especially within concrete research, has grown remarkably in recent years. This growth is motivated by the demand to enhance material performance, minimize experimental expenses, and accurately forecast concrete behavior under different conditions [58]. Recent research has confirmed the efficiency of AI methods in fulfilling these goals, representing a major advancement in the design and assessment of concrete mixtures [59]. In this experimental, waste ceramic tiles and silica nanoparticles derived from bottle glass were chosen for their abundance, affordability, and notable environmental advantages. As common by-products of construction and household waste, these materials help minimize landfill accumulation and support sustainable waste management practices. Their high silica content and amorphous characteristics enhance pozzolanic reactivity, contributing to a denser microstructure and greater concrete durability. The incorporation of these waste materials reduces cement usage and carbon emissions while offering a cost-effective and environmentally friendly solution for producing high-performance concrete. This research explores the utilization of WCTPs as a partial replacement for OPC (60 %) and crushed wastes tile ceramic (WTC) as a substitute for natural aggregates to enhance resistance against sulphuric acid and sulphate attacks. Furthermore, silica nanoparticles obtained from waste glass bottles (WBGNPs) were added at varying levels to accelerate early hydration and strengthen durability under aggressive conditions. The modified concrete was tested in 10 % H_2SO_4 and 10 % $MgSO_4$ solutions over exposure periods of 6 and 12 months. Performance evaluations included measurements of residual compressive strengths (RCS), weight losses (WL), ultrasonic pulse velocity (UPV), visual appearance, X-ray crystallography (XRD), field emission scanning electron microscopy (FESEM), energy dispersive X-ray analysis (EDX), and Fourier-transform infrared spectroscopy (FTIR) analyses.

2. Materials and methods

2.1. Characterizations of materials

In this study, waste tile ceramic materials were collected from the construction industry. The received materials were initially crushed using a Los Angeles Abrasion machine equipped with 25 stainless steel balls, each 40 mm in diameter, operating at a drum speed of 25–30 rpm (rpm). The crushed material was then sieved through a 600 μm sieve to remove larger particles, ensuring consistency in fineness by maintaining the same grinding procedure, duration, weight, and number of balls for each batch. The resulting fine powder was further ground for six hours until it passed through a 75 μm sieve, with fineness checked at one-hour intervals. The super-fine powder obtained was subsequently stored and used for mix design preparation.

For the production of silica nanoparticles, waste glass bottles collected from a local market were cleaned with tap water to remove dirt and impurities. The cleaned bottles were crushed using the Los Angeles Abrasion machine and sieved through a 600 μm sieve to separate coarse particles. The sieved glass was then ground for an additional three hours to achieve a particle size of approximately 25 μm. The resulting glass powder was annealed at (110 ± 5) °C for one hour and then subjected to a further seven hours of grinding using a ball milling machine to obtain a uniform distribution of glass nanoparticles.

Industrial waste materials, including WCTPs and WBGNPs, were prepared and used as partial replacements for OPC in concrete production (Fig. 1). Crushed ceramics served as replacements for fine and coarse aggregates. The materials were analyzed for their chemical composition, physical properties, morphology, and microstructure using methods such as Pycnometer testing [60], BET analysis [61], and particle size analysis (PSA) [62]. The OPC, meeting ASTM Type I cement standards (ASTM C150) [63], exhibited specific gravity (SG) of 3.15, a fineness of 3995 cm^2/g, and a median particle size of 16.4 μm, with 97 % of particles passing a 45 μm sieve.

X-ray fluorescence (XRF) spectroscopy was used to determine the chemical composition of the binder materials, including OPC, WTCPs, and WBGNPs.Table 1 outlines the OPC's chemical composition, highlighting its high calcium oxide (CaO) content, which enhances hydration reactions and early strength. The WCTP, after grinding, achieved a median particle size of 17.1 μm, with 97 % of particles below 45 μm, satisfying ASTM C618 pozzolanic requirements [64]. WCTP exhibited a specific surface area of 16.4 m^2/g, an SG of 3.06, and was primarily composed of silica and alumina oxides (85.6 %). Sodium oxide content (13.2 %) was identified as influential in hydration reactions. Transmission Electron Microscopy (TEM) analysis was employed to determine the median particle size of the nanomaterials. The results revealed that the WBGNPs had a median particle size of 80 nm, with a specific surface area of 206 m^2/g and a specific gravity of 1.02. The chemical composition of WBGNPs-derived silica nanoparticles revealed a high concentration of alumina and silica oxides (83 %), with both materials adhering to ASTM C618 standards.

Cleaned crushed granite stones were used as coarse aggregates in the concrete mixes, prepared and stored under saturated surface dry (SSD) conditions to minimize free-water content variations. As shown in Fig. 2, the grading of coarse aggregates followed ASTM C136 standards [65], with the granite aggregates exhibiting a specific gravity (SG) of 2.67, a water absorption rate of 1.2 % (ASTM C127), and a maximum particle size of 10 mm. Additionally, crushed ceramic aggregates, adhering to ASTM C33 specifications, were used as an alternative to natural aggregates, also with a maximum particle size of 10 mm.

For fine aggregates, river sand meeting ASTM C33 specifications [66] was used, with grading verified through sieve analyses in compliance with ASTM C136. The sand, maintained in SSD conditions as per ACI-219 standards, exhibited a specific gravity and water absorption capacity evaluated according to ASTM C128. The fineness modulus of the sand was determined to be 2.8, confirming its suitability for concrete mixes. Ceramic waste was also crushed and sieved to meet fine aggregate specifications in accordance with ASTM C33, successfully substituting natural sand in the designed concrete mixtures.

2.2. Mix design

The incorporation of high volumes of waste materials (up to 50 %) as partial cement replacements in concrete provides substantial sustainability advantages. These include improved durability in aggressive environments, reduced carbon emissions from cement production, conservation of natural resources, decreased energy demand, and the diversion of industrial by-products from landfills [57,68]. This approach aligns with the principles of the circular economy and promotes environmentally responsible construction practices. In this study, concrete

Fig. 1. Raw materials used in preparing the modified concrete specimens: (a) OPC, (b) WTCPs, (c) WBGNPs, (d) fine crushed ceramic ($\leq$ 4.75 mm), and (e) coarse crushed ceramic ($\leq$ 10 mm).

Table 1
Elemental weight percentages of the chemical compositions for OPC, WTCPS, and WBGNPs.

Composition	OPC	WTCPs	WBGNPs
SiO_2	17.60	71.7	69.14
Al_2O_3	4.54	13.9	13.86
Na_2O	2.49	13.21	8.57
Fe_2O_3	3.35	0.37	0.24
CaO	67.84	0.02	3.16
MgO	2.18	0.64	0.68
K_2O	0.27	0.03	0.01
LOI	1.73	0.13	0.16

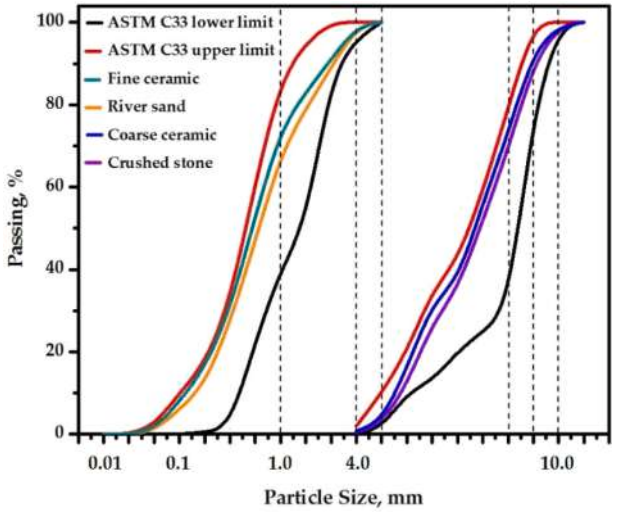

Fig. 2. Particle size distributions of river sand, crushed stones, and WTC aggregates (fine and coarse) in compared to ASTM C33 specifications [67].

was designed with 60 % WTCPs as a replacement for OPC. However, utilizing such a high proportion of WTCPs as a supplementary cementitious material often leads to slower early-age strength development due to its lower reactivity compared to OPC. The reduced early strength of WTCPs-modified concrete can restrict its use in construction applications that require rapid formwork removal, early load-bearing capacity, or accelerated construction timelines. To address this limitation, nanosilica derived from waste bottle glass has demonstrated significant potential in enhancing the early strength, durability, and sustainability performance of concrete. Owing to their ultra-fine particle size and large specific surface area, these nanoparticles accelerate hydration, leading to denser microstructures and improved early strength [69,70]. Such improvements contribute to the production of eco-friendly concrete by reducing cement consumption and encouraging the reuse of industrial waste, thereby supporting green construction initiatives. Considering these benefits, varying proportions of WBGNPs were incorporated into the cement matrix to develop high-performance concrete suitable for aggressive environments, as presented in Table 2.

The proposed binder was prepared by blending OPC, WTCPs, and WBGNPs for three minutes to achieve a homogeneous mix. The mixing process utilized a 0.2 m^3 drum mixer to ensure uniformity in the concrete mixtures. Initially, 50 % of the crushed ceramic aggregates were mixed for two minutes, followed by the addition of the remaining 50 %, which was blended for an additional three minutes in the dry state. Subsequently, the ternary blended binder, coarse aggregates, and fine aggregates were mixed in their dry state for five minutes. Water and a solution of superplasticizer (SP) were then added to activate the mix, which was further blended for four minutes before testing.

The workability of the fresh concrete was evaluated via slump tests as per ASTM C143, and the mix was poured into 100 mm $\times$ 100 mm $\times$ 100 mm steel molds following ASTM C579–18. The concrete was poured in layers, each compacted using a vibration table to minimize air voids and ensure uniformity. Mold surfaces were smoothed with a plasterer float. The prepared concrete specimens were maintained under laboratory conditions for 24 h at 26 $^{\circ}C \pm 1.5$ $^{\circ}$C and relative humidity above 75 %, followed by demolding and submersion in water for curing over a one-week period. The mixing and curing protocols ensured consistent concrete quality, as detailed in Table 2, supporting the evaluation of the designed mix's performance and durability.

2.3. Tests procedure

After 28 days of curing, the compressive strength of the modified

Table 2
Design of a sustainable concrete mix incorporating silica nanoparticles (kg/m³).

Mix code	Binder, kg/m³			WTC aggregates, kg/m³		Water to Binder	SP, %
	OPC	WTCPs	WBGNPs	Fine	Coarse		
100 % OPC	420	0	0	816	894	0.48	1.5
60 % WTCPs	168	252	0	816	894	0.48	1.5
2 % WBGNPs	168	252	8.4	816	894	0.48	1.5
4 % WBGNPs	168	252	16.8	816	894	0.48	1.5
6 % WBGNPs	168	252	25.2	816	894	0.48	1.5
8 % WBGNPs	168	252	33.6	816	894	0.48	1.5
10 % WBGNPs	168	252	42.0	816	894	0.48	1.5

concrete was tested to evaluate the influence of WTCPs–WBGNPs on concrete performance and to determine the optimal content. For each mixture, three concrete cubes were tested, and the average result was recorded. In compared to real environments, high concentration of sulphuric acid and sulphate (10 %) are used to accelerate the deterioration process which helps to simulate and predict the long-term performance of concrete within a shorter testing period (6–12 months). The effects of sulfuric acid on concrete specimens were assessed by immersing 28-day-old concrete samples in a 10 % H_2SO_4 solution prepared using deionized water [71]. Six specimens of each concrete type were evaluated, with specimens weighed before immersion and tested over a 365-day period. The acid solution was refreshed every 60 days to maintain stable pH conditions. Measurements were conducted at 180 days and one year, following ASTM C267 guidelines, to evaluate weight losses, residual compressive strength (RCS), and microstructural changes. For each age, three specimens were evaluated and the average value was considered. Sulfate attacks were primarily attributed to the infiltration of sulfate ions ($(SO_4)^{2-}$), which degraded the concrete by altering concentrations of magnesium (Mg), calcium (Ca), and sodium (Na) in the solution. Results indicated improved resistance of the concrete against sulfuric acid and magnesium sulfate solutions in harsh environments.

Microstructural analyses of acid-immersed specimens employed advanced techniques such as X-ray diffraction (XRD) [72], field emission scanning electron microscopy coupled with energy-dispersive X-ray spectroscopy (FESEM-EDX) [73], and Fourier-transform infrared spectroscopy (FTIR) [74]. XRD was utilized to identify crystalline phases, lattice parameters, and orientations in the mixes, with data collected over a 5–90° angle range at 0.02° increments. MDI Jade and Match software confirmed the amorphous characteristics of the specimens. High-magnification scanning electron microscopy (SEM) [75] analyzed surface morphologies of modified cement samples after one year of exposure. The samples for FESEM-EDX analysis were collected from the central portion of the cube immediately after the concrete specimens were crushed during the compressive strength test and were then promptly immersed in containers filled with acetone. Samples were mounted, dried, gold-coated, and imaged at 20 kV with 1000× magnification, providing critical insights into morphological changes. These observations underscore the improved durability of the modified concrete in aggressive environments.

3. Results and discussion

3.1. Workability and compressive strength

The effect of incorporating high volumes of WTCPs and varying content WGBNPs on the workability and compressive strength of concrete was evaluated. Workability was assessed using slump tests per ASTM C143, revealing that replacing 60 % of OPC with WTCPSs reduced slump values by 18.95 %, from 190 mm to 154 mm. The incorporation of WTCPs as a partial replacement for OPC decreases the slump and workability of concrete, primarily due to its angular particle shape, fine particle size, and limited water absorption capacity. These features increase internal friction and the total surface area within the mix, thereby demanding additional water to attain a similar flow to that of conventional concrete. Moreover, the ceramic powder lacks the smooth and lubricating nature of cement particles, resulting in a stiffer mix and reduced ease of placement and compaction [67].

Similarly, the addition of WGBNPs further decreased workability, with slump values decreasing by 3.24 %, 7.79 %, 10.38 %, 14.28 %, and 16.88 % as WGBNPs content increased from 0 % to 2 %, 4 %, 6 %, 8 %, and 10 %, respectively (Table 3). The incorporation of nanosilica into the cement matrix markedly decreases workability because of its ultrafine particle size and large surface area [76,77], which elevate water demand and particle friction. Nanosilica particles absorb a substantial portion of the mixing water, reducing the amount of free water available for lubrication. Moreover, their high pozzolanic reactivity accelerates the formation of calcium silicate hydrate (C–S–H) gels, further stiffening the mix. Consequently, the fresh paste becomes denser and less fluid, resulting in a significant reduction in workability [78].

Table 3 also highlights the impact of WGBNPs on the compressive strength of concrete over time. Incorporating WGBNPs at concentrations of 2 %, 4 %, 6 %, 8 %, and 10 % in the high-volume WTCPs mix (60 %) enhanced both early and long-term compressive strength. At 28 days, the compressive strength increased to 28.3, 36.9, 35.3, 31.1, and 26.9 MPa, surpassing the strength of the ceramic-based mix without nanoparticles (26.4 MPa). This improvement is attributed to the nanoparticles' ability to accelerate hydration, densify the gel matrix, reduce porosity, and refine the microstructure. The inclusion of nanomaterials facilitates filling and micro-aggregate effects, forming a denser and stronger cementitious matrix. Barbhuiya et al. [51] reported that the inclusion varying level in concrete matrix significantly can be enhance the strength properties.

3.2. Sulfuric acid resistance

3.2.1. Residual compressive strength

The residual compressive strength of concrete specimens exposed to 10 % sulfuric acid was assessed over 6 and 12 months to evaluate the strength and durability of the proposed concretes. As shown in Fig. 3, the RCS of all specimens decreased with prolonged exposure. Control specimens exhibited significant deterioration, with compressive strength dropping from 43.9 MPa at 6 months to 11.3 MPa at 12 months. In contrast, modified concretes containing high-volume WCTP and silica nanoparticles from WBGNPs demonstrated improved resistance. The 60

Table 3
Slump and compressive strength of modified concrete.

Tests	OPC 100 %	WTCPSs 60 %	WGBNPs				
			2 %	4 %	6 %	8 %	10 %
Slump, mm	190	154	149	143	138	132	126
Compressive strength, MPa	43.9	26.3	28.3	36.9	35.3	31.1	26.9
Strength standard deviation ±	2.4	1.3	2.1	1.9	1.4	1.8	2.2

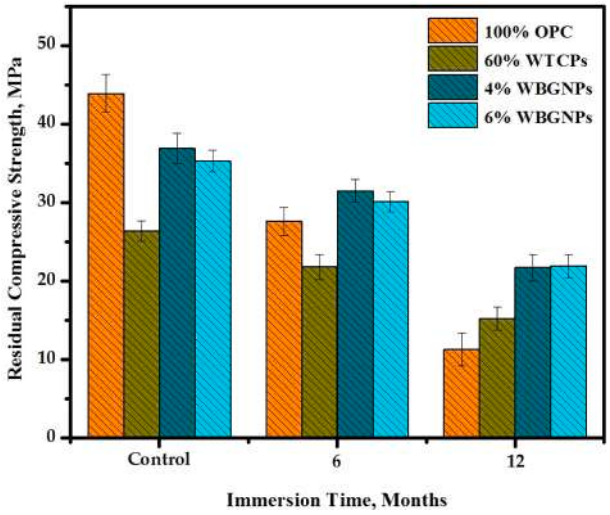

Fig. 3. Residual compressive strength of concrete specimens after immersion in the acid solution for 6 and 12 months.

% WCTP specimens showed a reduction from 26.4 MPa to 21.8 MPa at 6 months and further to 15.2 MPa at 12 months. Specimens containing 4 % WBGNPs exhibited better retention, with strength decreasing from 36.9 MPa to 31.5 MPa and 21.7 MPa over the same periods, while those with 6 % WBGNPs followed a similar trend, decreasing from 35.3 MPa to 30.1 MPa and 21.9 MPa. These findings highlight the superior acid resistance of modified concretes, attributed to the dense microstructure and reduced porosity provided by WTCP and WBGNPs.

Replacing 60 % of OPC with WTCPS and incorporating varying contents of WBGNPs significantly improved the resistance of concrete specimens to sulfuric acid attack, as illustrated in Fig. 4. After 6 months of immersion in a 10 % sulfuric acid solution, strength loss in the WCTP specimens was substantially reduced from 37.1 % to 14.7 % with the addition of 4 % and 6 % WBGNPs, respectively. Over a 12-month immersion period, control specimens with OPC showed severe deterioration, with strength loss reaching 74.3 %. In contrast, concrete specimens containing 60 % WCTP and supplemented with 4 % and 6 % WBGNPs exhibited significantly lower strength losses of 41.2 % and 37.9 %, respectively. These results demonstrate the effectiveness of WCTP and WBGNPs in enhancing acid resistance, reducing deterioration, and improving the durability of concrete in aggressive environments.

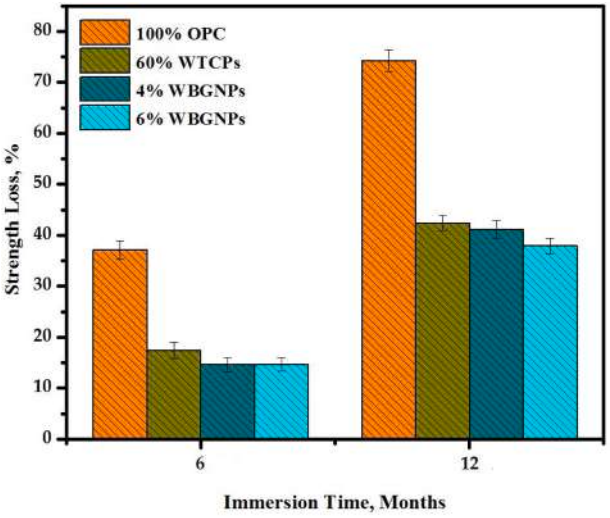

Fig. 4. Strength loss of proposed concrete specimens after immersion in acid solution for 6 months and 12 months.

The compressive strength loss of concrete exposed to sulfuric acid is primarily caused by the breakdown of the C-(A)-S-H gel and $CaCO_3$ network due to H^+ ions from H_2SO_4, which produce $Si(OH)_4$ and Al^{3+}. The enhanced resistance of modified concrete mixtures, containing 60 % WTCPS and 4–6 % WBGNPs, is attributed to their high silica and alumina content and reduced calcium hydroxide ($Ca(OH)_2$) due to pozzolanic reactions, which mitigate sulfuric acid attacks. In contrast, the degradation of OPC concrete is accelerated by significant gypsum formation from calcium-sulfuric acid reactions. The expansive pressure from gypsum increases cracking and microstructural damage, leading to greater strength loss in OPC concrete compared to the WTCPS-WBGNP mixtures, which exhibited improved durability and reduced deterioration.

The reactions outlined in Eqs. (1)–(3) describe the formation of gypsum (calcium sulphate dehydrate ($CaSO_4$. $2H_2O$)) and ettringite ($3CaO$. Al_2O_3. $3\ CaSO_4$. $32H_2O$) due to the interaction between sulphuric acid and cement hydration products, which are key factors contributing to sulphate attack in concrete [79]. In Eq. (1), sulphuric acid reacts with Portlandite ($Ca(OH)_2$) to produce calcium sulphate dihydrate, a compound that precipitates within the concrete's pore structure. Eq. (2) shows that sulphuric acid also attacks calcium silicate phases, leading to further gypsum formation along with the release of orthosilicic acid and water, thereby weakening the silicate matrix and increasing porosity. Subsequently, as described in Eq. (3), gypsum reacts with calcium aluminate phases ($3CaO$. Al_2O_3. $12H_2O$) in the presence of water to form ettringite, a highly expansive mineral. The continuous accumulation of gypsum and ettringite causes significant internal stress, volumetric expansion, and microcracking within the cement paste. Over time, these cracks facilitate deeper ingress of aggressive agents, accelerating deterioration, reducing structural integrity, and ultimately shortening the concrete's service life.

$$Portlandite + Sulphuricacid \rightarrow Calciumsulphatedihydrate \quad (1)$$

$$Calciumsilicate + Sulphuricacid \rightarrow Calciumsulphate + Orthosilicicacid + Water \quad (2)$$

$$Calciumaluminatemonosulfate + Calciumsulphatedehydrate + Water \rightarrow Ettringite \quad (3)$$

The chemical reactions depicted in Eqs. (1), 2, and 3 demonstrate that sulfuric acid deteriorates concrete through both sulfate and hydrogen ions, forming expansive byproducts such as gypsum and ettringite on the surface (Fig. 5). Gypsum, initially produced upon acid interaction, reacts with calcium aluminate phases in the cement matrix to generate ettringite, which further increases tensile stresses, leading to cracks and peeling. These byproducts are soft, movable, and gelatinous, resulting in the surface softening and degradation of the concrete specimens. This highlights the dual corrosive action of sulfuric acid and the role of expansive compounds in accelerating concrete deterioration.

3.2.2. *Weight loss*

Weight loss testing is a widely used method for assessing the degree of concrete degradation under sulfuric acid exposure due to its simplicity and convenience. As shown in Fig. 6, concrete weight loss increased with prolonged immersion in a 10 % H_2SO_4 solution over 6 and 12 months. Replacing 60 % of OPC with WCTP and incorporating varying amounts of WBGNPs reduced weight loss significantly. After 6 months, weight loss decreased from 4.97 % in control specimens to 4.52 %, 3.07 %, and 2.56 % with 60 % WCTP and 4 % and 6 % WBGNPs, respectively. A similar trend was observed at 12 months, where weight loss dropped from 15.35 % to 10.41 %, 8.33 %, and 8.12 %. The reduction in degradation was attributed to the lower CaO content in the modified matrix, limiting gypsum formation and reducing spalling and surface damage. As well as, the WTCP and WBGNPs help reduce the weight loss of concrete exposed to acid attack by producing a denser and

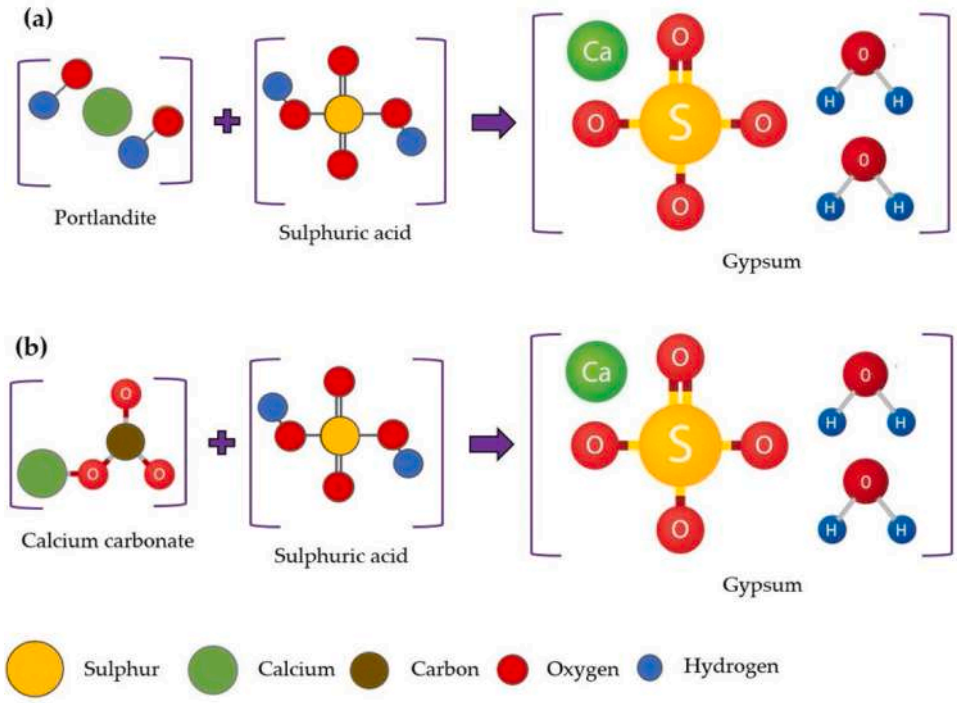

Fig. 5. Chemical formulation of gypsum ($CaSO_4 \cdot 2H_2O$) in concrete specimens exposed to a sulfuric acid (H_2SO_4) attack: (a) Reaction with portlandite ($Ca(OH)_2$); and (b) calcium carbonate ($CaCO_3$) process.

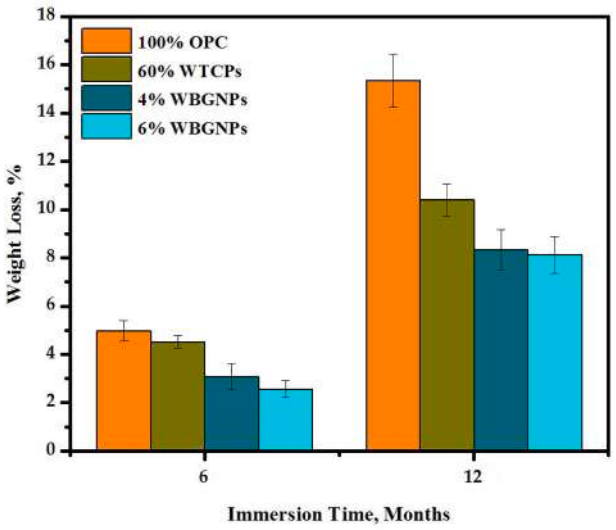

Fig. 6. Effects of 10 % H_2SO_4 acid solution exposure on the weight loss of concrete specimens immersed for 6 and 12 months.

less permeable microstructure through pozzolanic reactions and filler effects. These mechanisms limit the penetration of acidic substances into the concrete matrix. As a result, long-term durability is improved by generating more stable compounds and lowering the amount of reactive calcium hydroxide in the cement paste.

Initially, concrete specimens showed a slight weight gain during the first two to three months of immersion due to the reaction between sulfate ions (SO_4^{2-}) and hydration products, forming expansive compounds such as gypsum and ettringite, which filled porous spaces. Over time, however, the accumulation of these products caused internal stresses, cracking, and eventual weight loss. The pozzolanic reaction from WTCPs and WBGNPs substitution further improved durability by decreasing calcium hydroxide and increasing fine filler materials, enhancing resistance to sulfuric acid. These findings align with prior studies on the durability of pozzolanic material-modified concrete.

3.2.3. *Ultrasonic pulse velocity*

The effects of sulfuric acid on the internal structure of modified concrete specimens were assessed using ultrasonic pulse velocity (UPV) tests, as shown in Fig. 7. UPV readings demonstrated an increase in damage with prolonged exposure to a 10 % H_2SO_4 solution over 6 and 12 months. Control specimens made entirely with OPC showed the highest deterioration, with UPV values dropping from 4480 m/s at 6 months to 1482 m/s at 12 months, indicating extensive cracking and weakened interfacial transition zones (ITZ). In contrast, modified specimens containing 60 % WTCPs and 4 % or 6 % WBGNPs exhibited significantly improved resistance. After 6 months, UPV readings decreased only slightly, from 3692 m/s, 4410 m/s, and 4376 m/s to 3118 m/s, 3799 m/

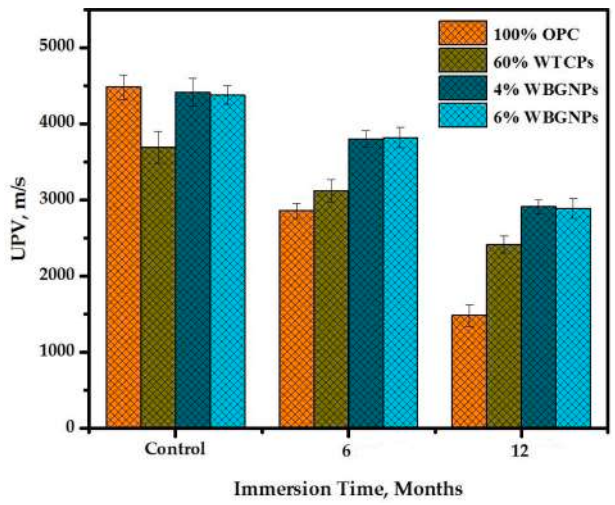

Fig. 7. UPV readings of modified concretes containing WCTP and WBGNPs after exposure to 10 % H_2SO_4 for 6 and 12 months.

s, and 3817 m/s, respectively, with similar trends observed at 12 months. The enhanced performance of the modified specimens is attributed to reduced CaO content and increased SiO_2, Al_2O_3, and MgO levels from the pozzolanic materials, which limited gypsum and ettringite formation, improving structural stability against sulfuric acid attack.

Prolonged exposure to the sulfuric acid environment caused gradual but progressive deterioration of concrete, characterized by gypsum formation and subsequent ettringite production. These expansive compounds led to micro-cracking, spalling, and strength loss due to internal stress and bond weakening within the matrix. The C-S-H and C-A-S-H gels underwent decalcification, transforming into hydrous silica, further reducing matrix cohesiveness and bond strength. Visual inspections noted a whitish gypsum layer on specimen surfaces after initial exposure, with degradation becoming more pronounced over time, especially for OPC specimens. However, modified specimens benefited from enhanced pore-filling and pozzolanic reactions from WCTPs and WBGNPs, mitigating the effects of acid attack. These findings align with prior studies correlating compressive strength and UPV, underscoring the durability advantages of incorporating sustainable replacement materials.

3.2.4. *Visual appearance*

Visual inspection of concrete specimens exposed to sulfuric acid for 12 months revealed significant differences in surface deterioration among the tested mixes, as shown in Fig. 8. Control specimens made with 100 % OPC exhibited severe surface damage and extensive crack formation (Fig. 8a), whereas the modified specimens with WTCPs and WBGNPs showed improved durability. Specimens incorporating 60 % WTCPs and 6 % WBGNPs demonstrated the highest resistance to acid attacks, with minimal surface damage and reduced crack formation (Fig. 8d). Acid attack on concrete primarily results in surface paste loss, aggregate degradation, and gypsum formation due to the reaction of sulfuric acid with calcite and Portlandite. Gypsum, a weak and moisture-sensitive compound, forms a white, sticky layer that erodes over time, causing spalling and material loss. The enhanced resistance in the modified mixtures is attributed to the nanoparticles' ability to improve compactness, reduce gypsum formation, and slow the rate of material deterioration, thereby extending the concrete's service life.

The enhanced resistance of modified concrete specimens containing 60 % WTCPS as a replacement for OPC and supplemented with WBGNPs can be attributed to the formation of dense gels such as C-(A)-S-H and $CaCO_3$ with a low CaO to SiO_2 ratio (0.54). In acidic environments, these dense gels release lime, leaving behind a protective silica and aluminosilicate gel layer that shields the cement paste from further corrosion. In contrast, OPC specimens, with a high CaO to SiO_2 ratio (3.85), experience dissolution of calcium hydroxide and calcium sulphoaluminates, leading to decalcification of dense C-S-H gels and forming a porous, degraded layer vulnerable to sulfuric acid attacks. The inclusion of WBGNPs as supplementary cementing materials further enhances durability by promoting a lower CaO to SiO_2 ratio and forming a dense silica gel layer, effectively protecting the modified cement paste against degradation.

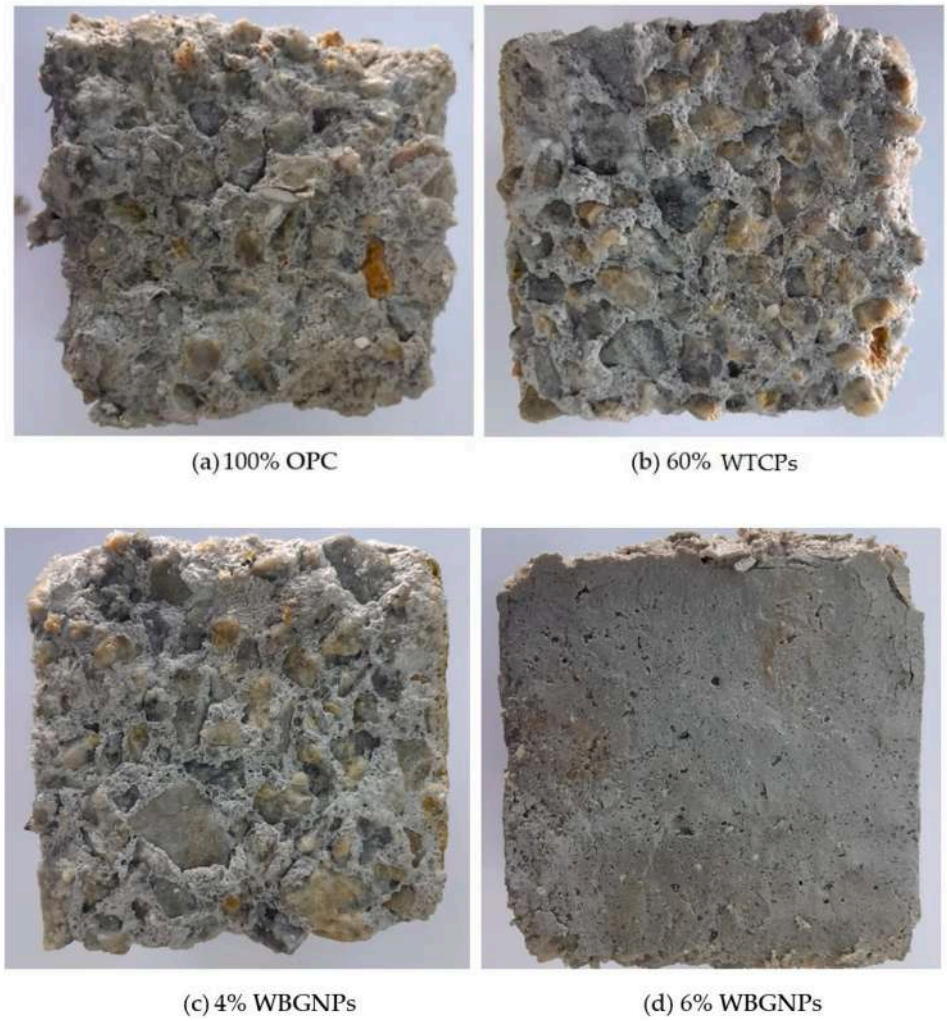

Fig. 8. Visual appearance of concrete specimens after 12 months of acid solution exposure: (a) 100 % OPC, (b) 60 % WTCPs, (c) 4 % WBGNPs, and (d) 6 % WBGNPs.

3.2.5. X-Ray diffraction (XRD)

The analysis of four modified concrete mixtures revealed a significant reduction in gypsum formation when 60 % of OPC was replaced with WCTPs and 4–6 % WBGNPs, as indicated by the lower intensity of gypsum peaks at key diffraction angles, including 29.6° 2theta (Fig. 9). The inclusion of WCTP and WBGNPs shifted diffraction peaks from 29.7° to 31.4°, supporting reduced gypsum and ettringite generation and enhancing resistance to sulfuric acid attacks.

Table 4 shows that control specimens with 100 % OPC exhibited higher gypsum (20.5 %) and ettringite (34.7 %) formation compared to modified concretes, which ranged from 14.8 to 15.3 % for gypsum and 23.9–24.8 % for ettringite. The higher OPC content in control specimens led to increased calcium hydroxide availability, resulting in more gypsum and ettringite formation, causing internal stresses, micro-cracking, and structural deterioration. Conversely, the reduction in OPC content in the modified mixes limited calcium hydroxide production, improving durability against sulfuric acid. This highlights the role of WTCPs and WBGNPs in mitigating gypsum formation, reducing cracking, and enhancing concrete resistance in acidic environments.

In sulfuric acid environments, Portlandite in the concrete matrix reacts with the acid to form gypsum, which detaches from the structure, increasing porosity and reducing compressive strength. Prolonged exposure exacerbates strength loss as gypsum reacts with Tricalcium aluminate and water, forming expansive ettringite. This reaction induces internal pore pressure, leading to crack formation and secondary corrosion. The deterioration of concrete strength and durability is further linked to a higher calcium-to-silica ratio and extended exposure to acidic conditions, underscoring the critical role of material composition in resisting acid attacks.

3.1.7. FESEM image analysis

The effects of sulfuric acid on the surface morphology of concrete specimens were analyzed using FESEM after 12 months of immersion in a 10 % H_2SO_4 solution, with results shown in Fig. 10. The SEM micrographs of control specimens made with 100 % OPC (Fig. 10a) revealed extensive gypsum and ettringite formation, larger crystal sizes, and numerous micro-cracks and pores compared to the modified concrete specimens containing WTCPS and WBGNPs (Figs. 10b, c, and d). The control specimens exhibited highly porous surfaces with decomposed C-S-H and C-A-S-H gels, Portlandite remnants, and unreacted quartz, leading to surface spalling and disintegration. In contrast, modified specimens demonstrated reduced gypsum and ettringite formation,

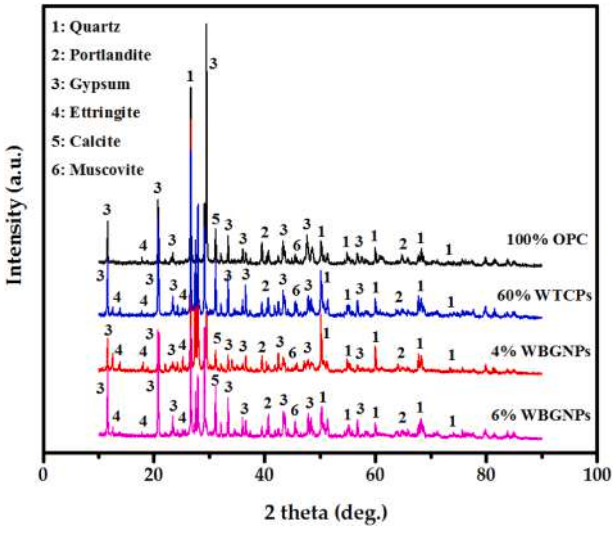

Fig. 9. XRD patterns of modified concrete specimens containing 100 % OPC, 60 % WCTPs, 4 % WBGNPs, and 6 % WBGNPs after 12 months of exposure to the acid solution.

Table 4
X-ray diffraction (XRD) peak analysis of concrete specimens after 12 months of immersion in a 10 % H_2SO_4 solution.

Indices	Amount, weight %				
	Gypsum	Ettringite	Portlandite	Quartz	Others
100 % OPC	20.5	34.7	17.2	27.6	1.7
60 % WTCPs	15.1	24.8	16.9	40.6	2.6
4 % WBGNPs	15.3	24.3	17.1	41.2	2.1
6 % WBGNPs	14.8	24.9	16.7	42.7	1.9

fewer micro-cracks, and improved surface morphology. The sulfate ions from sulfuric acid degraded the dense C-(A)-S-H gels on the concrete's surface, increasing porosity and accelerating deterioration. Increased exposure time amplified micro-crack formation and porosity, weakening the cohesiveness of the concrete and reducing residual compressive strength. The results highlight the superior resistance of modified concretes to sulfuric acid attacks due to the incorporation of WTCPs and WBGNPs.

3.1.8. Energy dispersive X-Ray analysis (EDX)

The EDX atomic spectrum analysis (Fig. 11) revealed significant changes in the microstructure and elemental composition of concrete specimens exposed to sulfuric acid for one year, highlighting the leaching of CaO and Al_2O_3. Control specimens displayed higher calcium (29.3 %) and sulfur (4.6 %) contents, indicating extensive ettringite and gypsum formation, consistent with FESEM and XRD findings. Conversely, modified concretes with 60 % WTCPS and 4–6 % WBGNPs showed reduced calcium (21.6 %, 21.4 %, and 19.1 %) and sulfur (1.6 %, 1.4 %, and 0.5 %) levels, reflecting lower gypsum and ettringite crystallization. These reductions correlate with increased resistance to sulfuric acid attacks. Silica content in modified specimens was higher (7.3 %) compared to controls (5.4–6.4 %), signifying greater C-S-H and C-A-S-H gel dissolution and transformation into a crystalline solid. The findings confirm that incorporating WTCPs and WBGNPs mitigates ettringite and gypsum formation, reduces internal stresses, and enhances concrete durability in acidic environments, aligning with prior studies.

3.1.9. FTIR spectral analysis of concrete

The FTIR spectra of modified concrete specimens exposed to a 10 % H_2SO_4 solution for one year (Fig. 12) revealed distinct vibration modes associated with Al-O, Si-O-Si/Al, Al-OH, Si-O of C-S-H gels, and C—O of calcite, among others, indicating chemical changes due to acid exposure. Control specimens with 100 % OPC exhibited more pronounced asymmetric Si-O-Si and Al stretching vibrations (1137–1091 cm^{-1}), corresponding to higher levels of calcium-rich ettringite and gypsum formation compared to modified specimens containing 60 % WCTP and 4–6 % WBGNPs. Vibrations linked to gypsum crystals were detected in all specimens at 662–658 cm^{-1}, while strong C—O stretching vibrations in control specimens (1413.9 cm^{-1}) were slightly reduced in modified specimens (1412.6–1412.1 cm^{-1}). Additionally, the range of 3610–3440 cm^{-1} highlighted hydroxyl group bonds in all acid-exposed samples, suggesting de-alumination and breakdown of the Al_2O_3-SiO_2 network due to reactions with sulfur. These findings, supported by XRD, FESEM, and EDX analyses, demonstrate that the incorporation of WTCPs and WBGNPs reduces ettringite and gypsum formation, improving resistance to sulfuric acid attacks.

3.3. Sulphate acid resistance

3.3.1. Specimens' strength performance

The strength of concrete exposed to a 10 % $MgSO_4$ solution was evaluated over 6 and 12 months, with strength loss percentages shown in Fig. 13. Strength loss increased with longer exposure, with control specimens (100 % OPC) exhibiting the highest losses: 8.04 % after 6

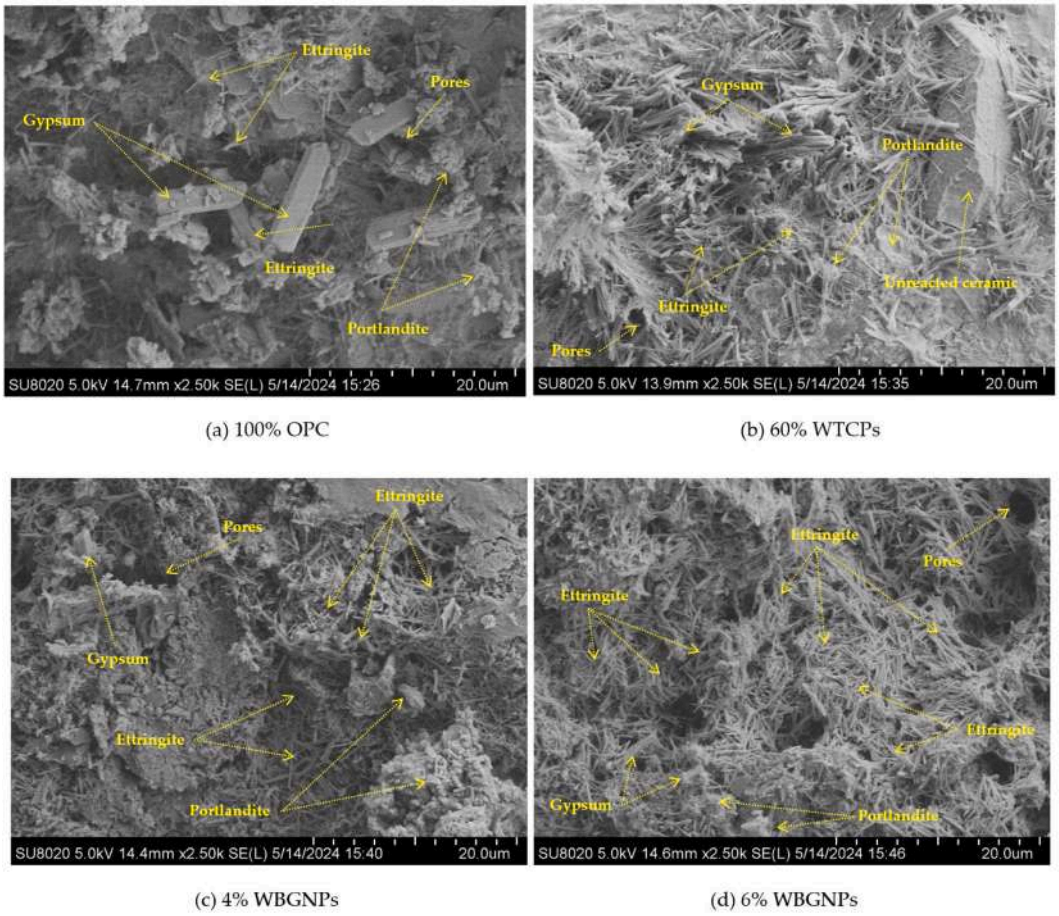

Fig. 10. Surface morphology of modified concrete specimens after 12 months of exposure to 10 % H_2SO_4 solution: (a) 100 % OPC, (b) 60 % WTCPs, (c) 4 % WBGNPs, and (d) 6 % WBGNPs.

months and 15.17 % after 12 months. In contrast, specimens incorporating 60 % WTCPs and 4 % or 6 % WBGNPs demonstrated significantly improved resistance, with strength losses of 1.74 %, 1.59 %, and 0.99 % at 6 months, and 5.98 %, 2.82 %, and 1.45 % at 12 months, respectively. These improvements are attributed to reduced calcium hydroxide content, which limits the formation of gypsum and ettringite, compounds known to cause expansion, micro-cracking, and accelerated deterioration in aggressive sulfate environments. The replacement of OPC with WTCPs and WBGNPs effectively mitigates these degradation mechanisms, enhancing the durability of concrete under sulfate attack. The inclusion of pozzolanic materials incorporating nanoparticles significantly enhance the durability performance of proposed concrete and reduce strength loss in specimens exposed to acid attack by producing a denser microstructure that lowers permeability and limits the penetration of harmful ions. In addition, SCMs react with calcium hydroxide, a byproduct of cement hydration, to generate extra binding phases such as calcium silicate hydrate (C-S-H) and calcium aluminate silicate hydrate (C-A-S-H), which enhance long-term strength and durability.

3.3.2. *Weight loss*

Fig. 14 depicts the weight loss percentage of concrete specimens prepared with high amounts of WTCPs and WBGNPs exposed to sulfate attacks. A direct correlation between weight loss and exposure time was observed across all specimens. The replacement of 60 % OPC with WCTP and the incorporation of 4 % and 6 % WBGNPs significantly enhanced concrete durability, reducing weight loss during immersion in a 10 % $MgSO_4$ solution. After 6 months, weight loss decreased from 1.24 % (control) to 0.45 %, 0.43 %, and 0.41 % for specimens containing 60 % WTCPs and 4 % or 6 % WBGNPs, respectively. Similar improvements were observed after 12 months, with weight loss reduced from 3.32 % to 2.23 %, 1.75 %, and 1.69 %. These reductions are attributed to lower calcium hydroxide content, which limits gypsum and ettringite formation, mitigating expansion and micro-cracking, and enhancing durability against aggressive sulfate environments.

3.3.3. *Ultrasonic pulse velocity*

Fig. 15 shows the UPV readings of proposed concretes before and after exposure to sulfate attacks for 6 and 12 months, demonstrating a decrease in UPV values with longer exposure, indicating the formation of micro-internal cracks due to gypsum and ettringite expansion. Control specimens made with 100 % OPC exhibited rapid deterioration, with UPV readings dropping from 4480 m/s to 3986 m/s after 6 months and to 3068 m/s after 12 months. In contrast, modified specimens containing 60 % WTCPs and 4 % or 6 % WBGNPs showed improved resistance, with UPV reductions from 3692 m/s to 3418 and 3106 m/s, from 4410 m/s to 4302 and 4089 m/s, and from 4376 m/s to 4252 and 3994 m/s, respectively. These results highlight the superior durability of modified concretes under sulfate attack due to reduced gypsum and ettringite formation.

3.3.4. *X-Ray diffraction (XRD)*

Fig. 16 illustrates the XRD analysis of modified concrete specimens exposed to 10 % sulfuric acid for 12 months, showing the presence of gypsum in all tested mixtures. The intensity of gypsum peaks at key angles, including 29.6° 2θ, decreased significantly with the replacement of 60 % OPC by WTCPs and the addition of 4 %−6 % WBGNPs. Peaks at 10.8°, 21.1°, 34.8°, 48.9°, and 56.9° also demonstrated reduced intensity, indicating limited gypsum and ettringite formation in the

modified concrete. The double peak structure at 27.6° and 27.9° suggested the coexistence of quartz and gypsum, corroborating previous findings by Bellmann and Stark. The shift in peak from 29.7° to 31.4° in modified specimens further supports enhanced resistance to sulfuric acid. Reduced OPC content in the binder matrix minimizes free calcium hydroxide, which is prone to sulfate attack, thereby improving the durability of the modified concrete.

3.3.5. FESEM image analysis

Fig. 17 presents the FESEM analysis of concrete specimens exposed to 10 % $MgSO_4$ solution for 12 months, highlighting the effects of sulfate attacks on surface morphology. Control specimens made with 100 % OPC (Fig. 17a) exhibited severe deterioration, characterized by larger quantities and sizes of gypsum and ettringite crystals compared to modified specimens containing 60 % WTCPs and 4 %–6 % WBGNPs. The control specimens also displayed more micro-cracks and higher porosity, leading to increased internal stresses and expansion, which significantly contributed to strength, weight, and UPV losses. In contrast, the modified specimens demonstrated improved durability with reduced gypsum and ettringite formation, fewer cracks, and lower porosity, underscoring the enhanced resistance of WCTPs- and WBGNPs-enriched concrete against sulfate attacks.

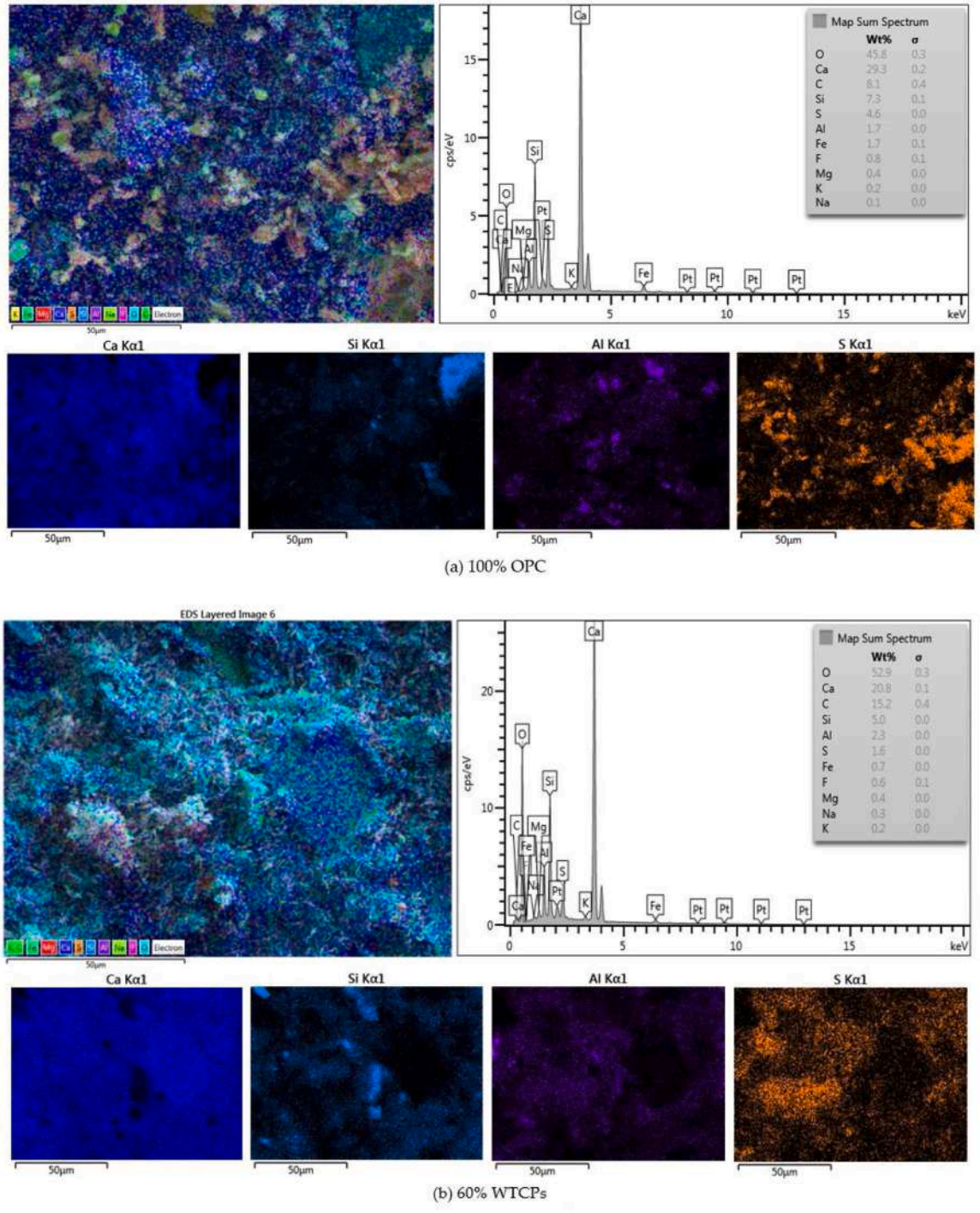

Fig. 11. EDX spectral analysis of modified concrete specimens after one year of exposure to 10 % H_2SO_4 solution: (a) 100 % OPC, (b) 60 % WTCPs, (c) 4 % WBGNPs, and (d) 6 % WBGNPs.

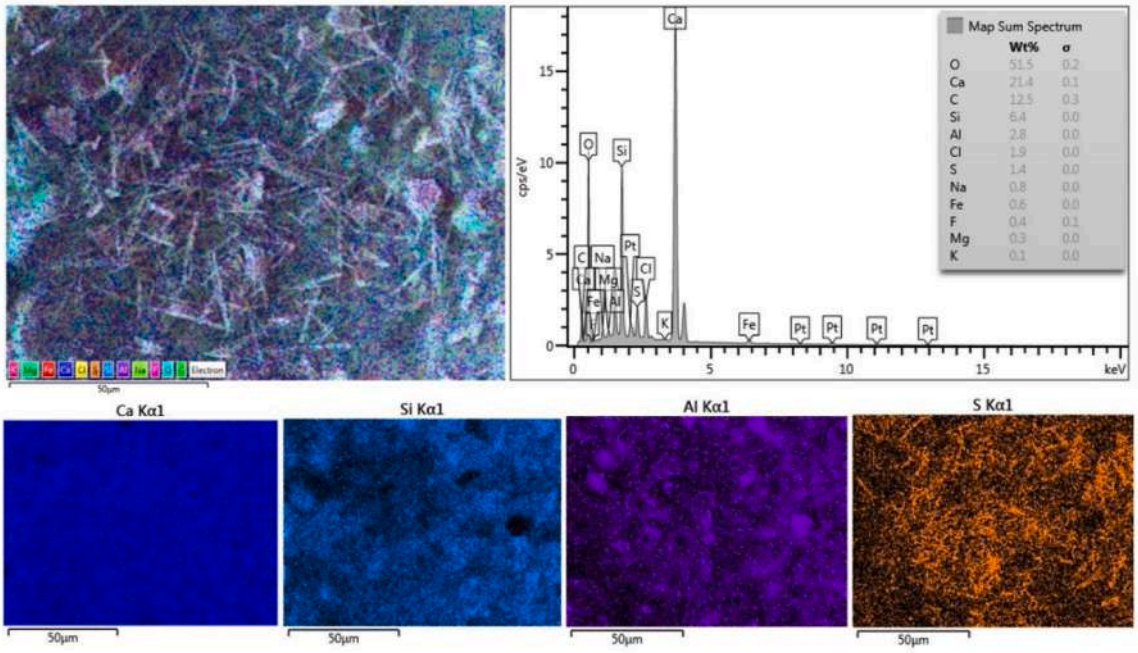

(c) 4% WBGNPs

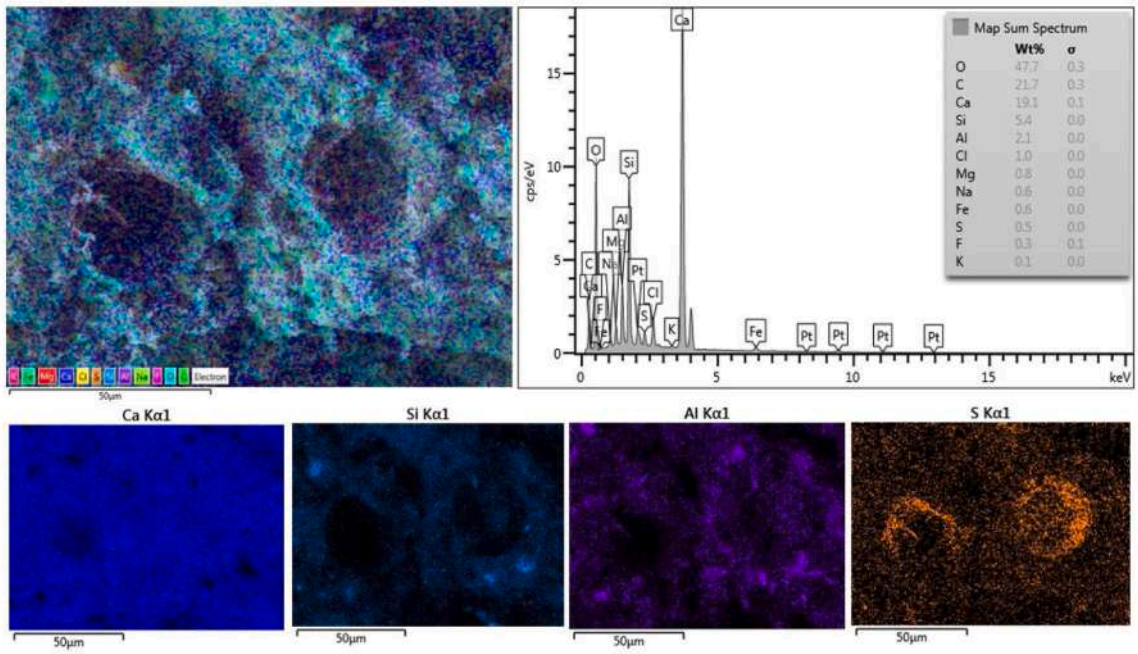

(d) 6% WBGNPs

Fig. 11. (*continued*).

3.3.6. *FTIR spectral analysis of concrete*

Fig. 18 shows the FTIR spectra of modified concrete specimens exposed to sulfate attacks for 12 months, revealing the chemical and structural changes in the binder due to prolonged exposure. Significant stretches, including Al-O, Si-O-Si/Al, Al-OH, Si-O of C-S-H gels, C—O of calcite, and O—H of water, reflect the influence of binder composition and sulfate exposure. The Si-O-Al, O—H, and C—O stretches observed in the spectra indicate the dealumination of the Al_2O_3-SiO_2 network resulting from the reaction between calcium hydroxide and external sulfur. These findings, corroborated by XRD, FESEM, and EDX analyses, confirm the formation of gypsum and ettringite crystals, highlighting the degradation mechanisms affecting concrete durability under sulfate attacks.

4. Application of AI for estimation and optimization

In this section, artificial intelligence (AI) was employed to estimate and optimize the concrete mix design for minimizing strength and weight loss under acidic and sulphate environments. A Random Forest Regressor model [80] was developed using experimental data to predict degradation outcomes based on various mix parameters, including OPC, WTCPS, and WCT aggregate, the Sequential Least Squares Programming

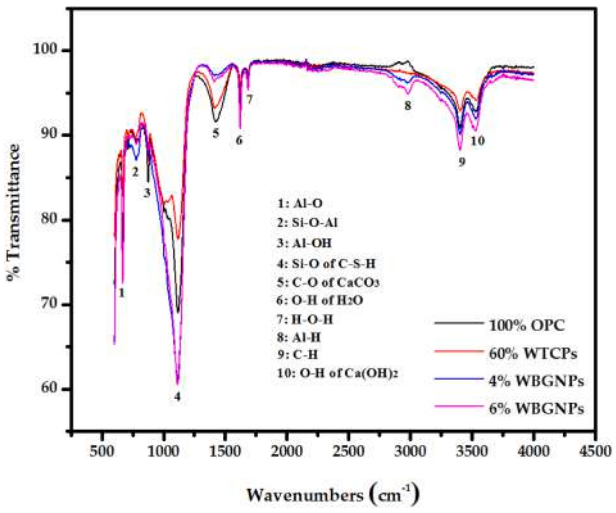

Fig. 12. FTIR analysis of modified concretes containing high volumes of WTCPs and WBGNPs after 12 months of exposure to 10 % H_2SO_4.

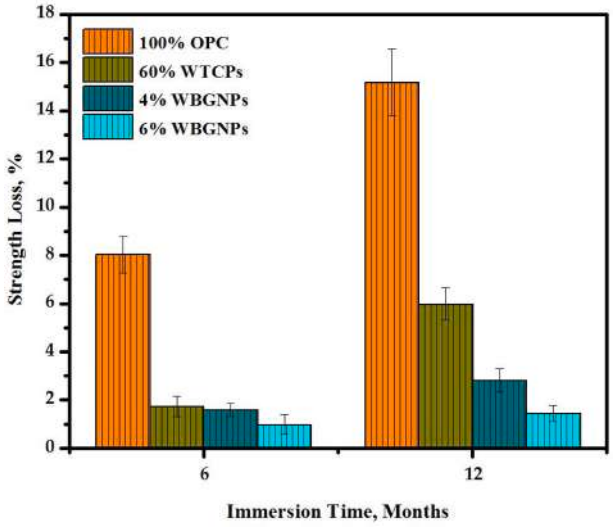

Fig. 13. Strength loss percentage of proposed concrete specimens exposed to 10 % $MgSO_4$ solution for 6 and 12 months.

(SLSQP) algorithm [81] was applied to optimize these parameters, incorporating constraints to ensure the total weight of aggregates did not exceed 1700 kg/m^3. This AI-driven approach not only enhanced the accuracy of the predictions but also facilitated the identification of an optimal mix design that significantly reduces concrete deterioration, demonstrating the efficacy of integrating machine learning techniques in civil engineering applications.

4.1. Dataset and correlation matrix

In the provided correlation matrix, the relationship between various construction material properties is quantified, with a color gradient ranging from blue (indicating a strong negative correlation) to red (indicating a strong positive correlation). Notably, WCT aggregate_Coarse and WCT aggregate_Fine exhibit a perfect correlation coefficient of 1.00, suggesting identical or highly related measures. Moreover, variables such as Acid Strength Loss and Sulphate Strength Loss over 6 and 12 months show strong negative correlations with OPC, highlighting a significant inverse relationship. Additionally, the SP_Percent variable demonstrates moderate positive correlations with W_C and OPC, indicating potential interactions that could influence the hydration and setting characteristics of concrete (Fig. 19).

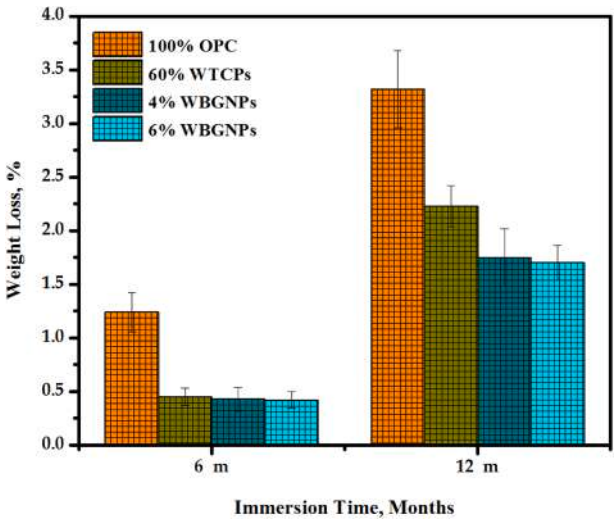

Fig. 14. Weight loss of proposed concrete specimens exposed to 10 % $MgSO_4$ solution for 6 and 12 months.

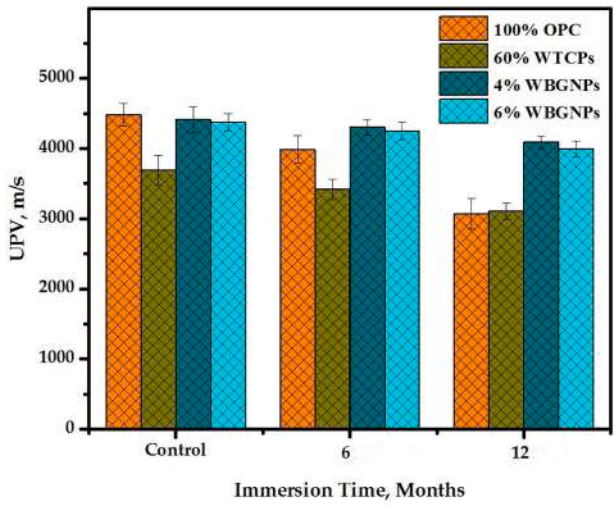

Fig. 15. UPV readings of proposed concrete exposed to sulfate attacks for 6 and 12 months.

4.2. Performance prediction

The prediction of strength and weight loss in concrete subjected to acidic and sulphate environments was performed using a Random Forest regression model. This ensemble learning algorithm effectively captures complex, non-linear relationships among the input parameters and their effects on performance metrics. The model was trained to minimize the mean squared error (MSE), defined as:

$$MSE = \frac{1}{n}\sum_{i=1}^{n}(y_i - \hat{y}_i)^2 \quad (4)$$

where y_i represents the actual values and $\hat{y}_i$ denotes the predicted values. The Random Forest model combines the predictions from multiple decision trees, enhancing robustness and accuracy. After training, the model was validated on a separate test set, allowing for precise predictions of strength and weight loss over a 12-month period. This predictive capability served as a foundation for the optimization of the concrete mix design, ensuring enhanced performance in aggressive environmental conditions.

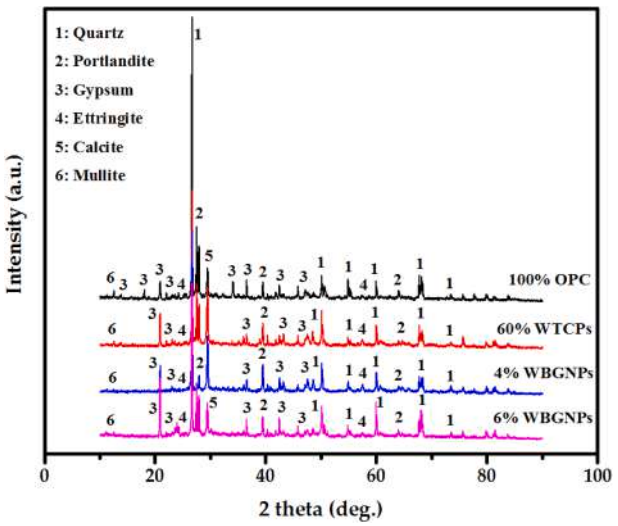

Fig. 16. XRD analysis of proposed concrete specimens after 12 months of exposure to sulfate attacks.

Fig. 20 presents the comparison between actual and predicted values for Acid and Sulphate Strength Loss, as well as Acid and Sulphate Weight Loss, all measured over a 12-month period. Each subplot demonstrates a strong linear relationship between the actual and predicted data, with high coefficients of determination (R^2 values) ranging from 0.97 to 0.99. This indicates that the predictive model provides an accurate estimation of both strength and weight loss under acidic and sulfate conditions. The close alignment of the data points with the linear regression line further confirms the model's ability to replicate the experimental results with minimal deviation, validating its reliability for forecasting long-term performance in similar environmental conditions.

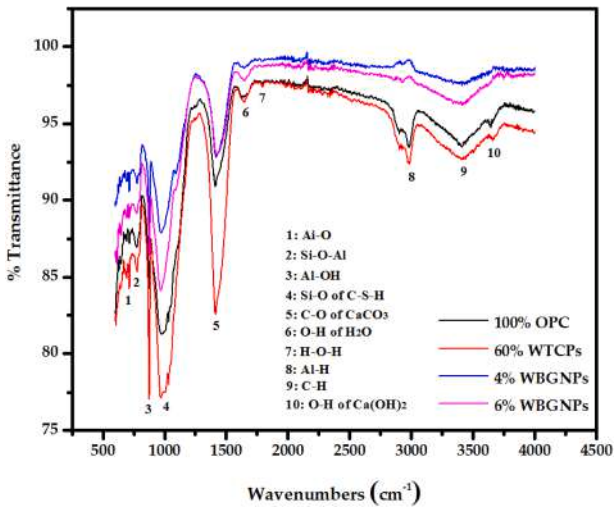

Fig. 18. FTIR analysis of proposed concrete specimens after 12 months of exposure to sulfate attacks.

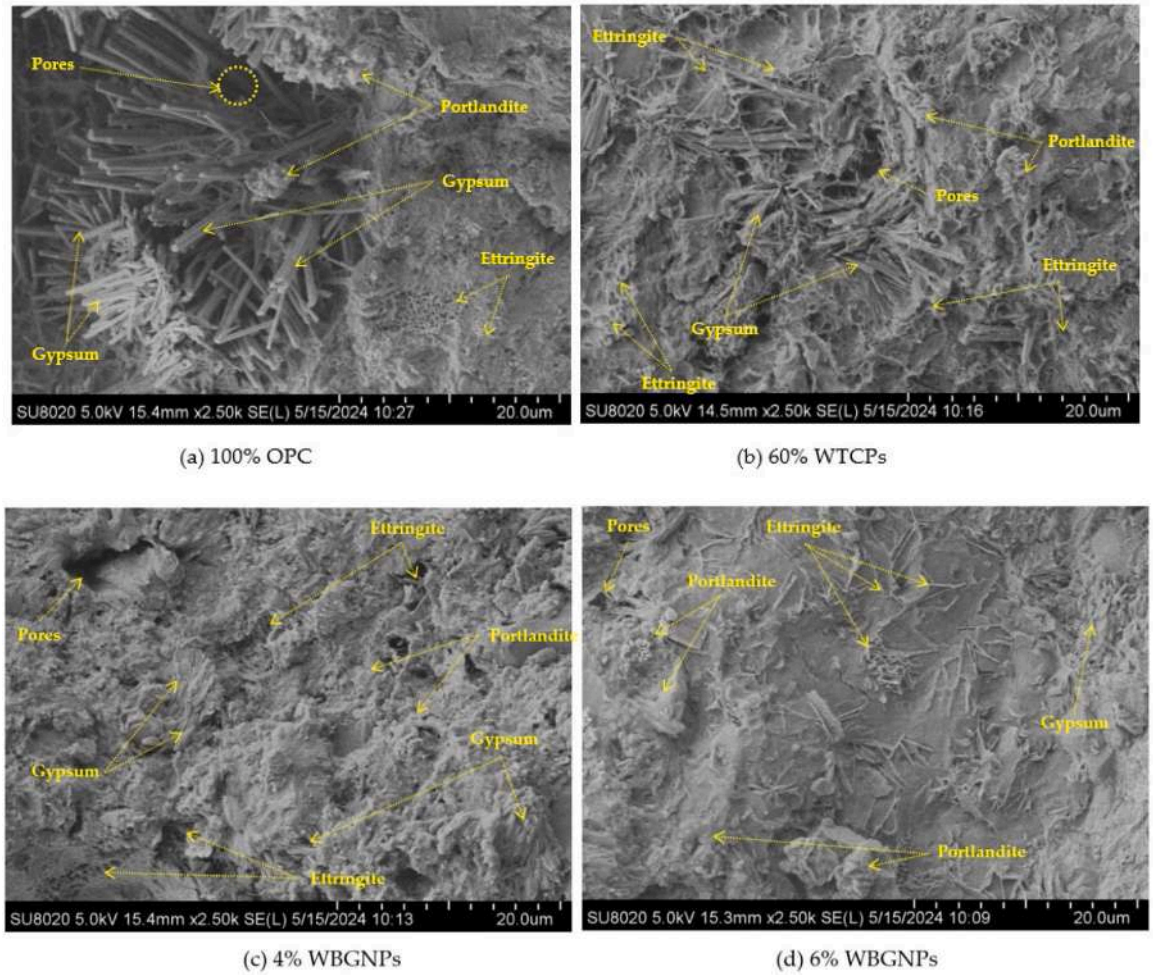

Fig. 17. FESEM images of proposed concrete after 12 months of exposure to sulfate attacks.

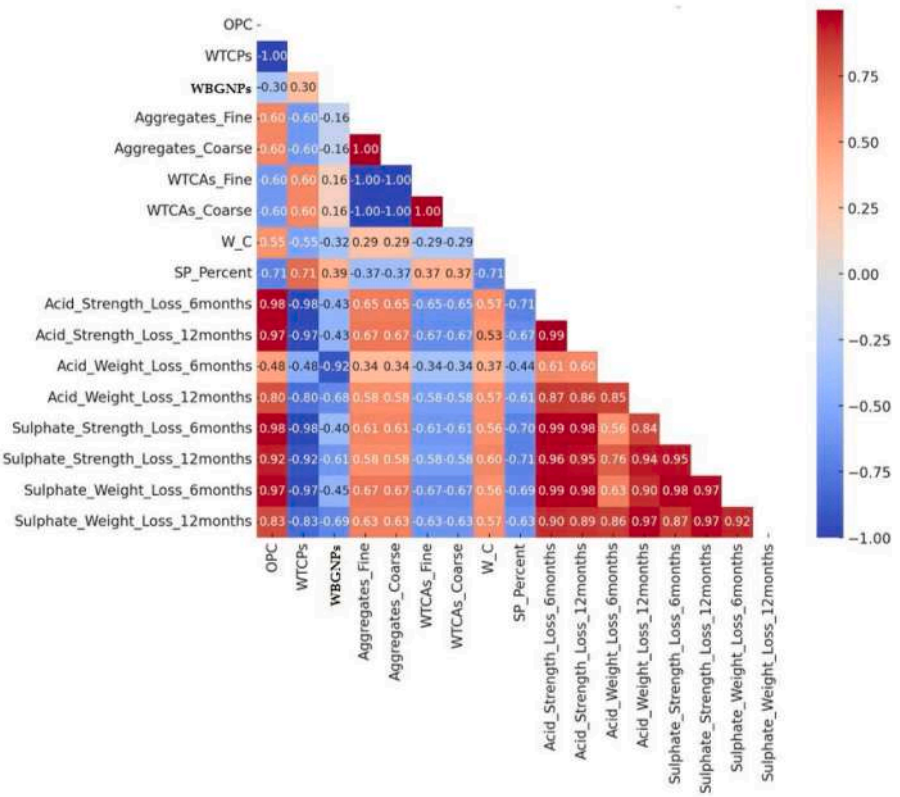

Fig. 19. Correlation matrix showing the relationships between concrete properties.

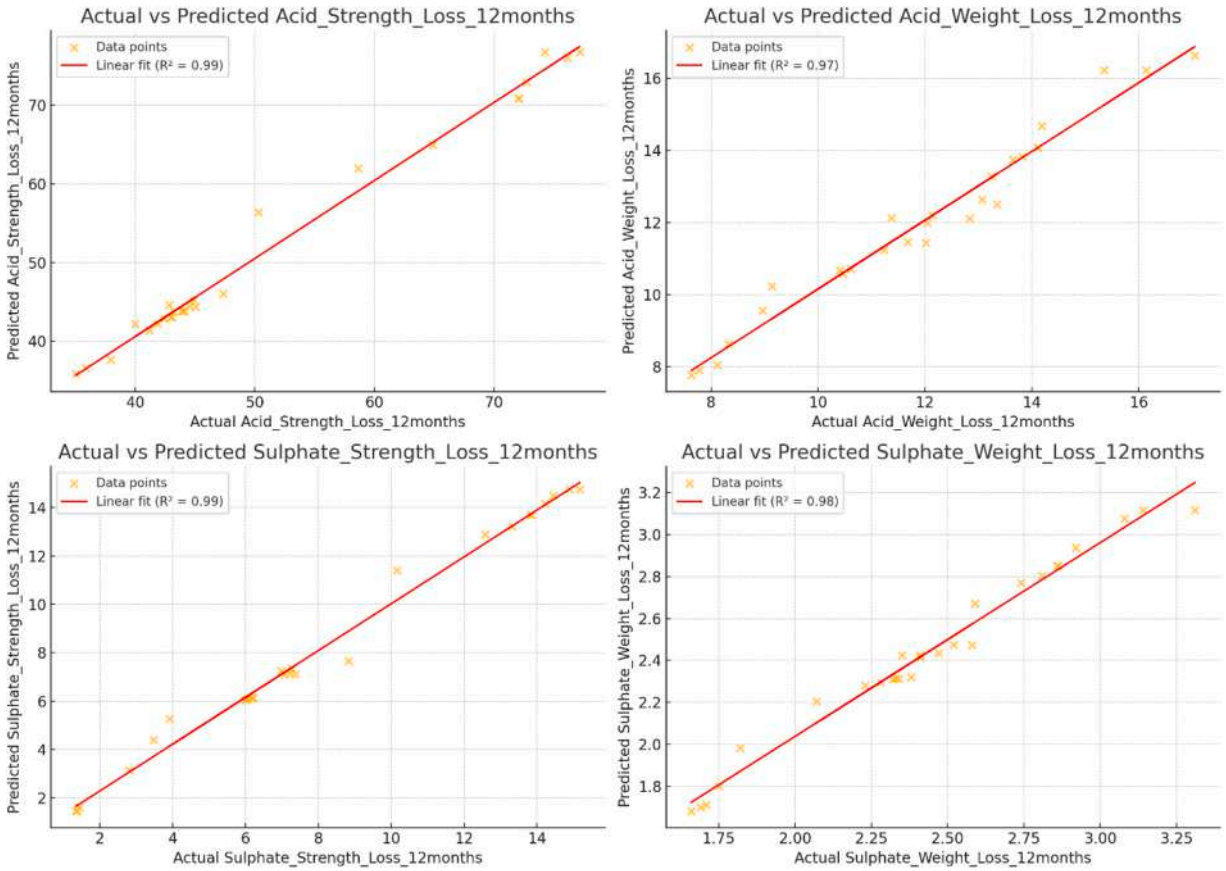

Fig. 20. Actual and predicted values for Acid and Sulphate Strength Loss.

Table 5 summarizes the performance metrics of the predictive model for four output parameters: Acid Strength Loss, Acid Weight Loss, Sulphate Strength Loss, and Sulphate Weight Loss, all measured over 12 months. The model demonstrates high accuracy, as evidenced by the high R^2 values (ranging from 0.97 to 0.99), which indicate strong correlations between predicted and actual values. The Mean Squared Error (MSE) and Mean Absolute Error (MAE) values are also provided, where lower values indicate better model performance. The model exhibits the best performance in predicting Sulphate Weight Loss, with the lowest MSE (0.01) and MAE (0.08), while maintaining strong accuracy across all parameters. These results highlight the model's reliability in forecasting long-term deterioration under acid and sulfate exposure.

The following equations have been extracted from an AI-driven model, specifically designed to predict the strength and weight loss of concrete after 12 months under acid and sulphate resistance. These equations offer a high degree of accuracy, with the models for sulphate resistance achieving R^2 values of 0.949 and 0.842 for strength and weight loss, respectively, indicating strong predictive power. Although the model for acid weight loss requires further refinement, the overall results demonstrate the potential of AI in enhancing decision-making processes in concrete mix design and performance evaluation. By integrating these AI-derived equations into engineering workflows, professionals can better estimate concrete durability under various environmental conditions, facilitating more informed and efficient decision-making in the field of sustainable construction.

Acid Resistance

Strength Loss:

$$\begin{aligned} Acid\ Strength\ Loss\ =\ & 6.26 * OPC - 6.26 * WCTPs - 2.52 \\ & * WBGNPs - 36.43 * Fine\_NA + 37.34 \\ & * Coarse\_NA + 36.43 * Fine\_WTC\ agg \\ & - 37.34 * Coarse\_WTC\ agg + 0.08 * W/C \\ & + 0.61 * SP + 51.18 \end{aligned} \quad (5)$$

Weight Loss:

$$\begin{aligned} Acid\ Weight\ Loss\ =\ & 0.83 * OPC - 0.83 * WCTPs - 1.23 \\ & * WBGNPs + 49.11 * Fine\_NA - 48.83 \\ & * Coarse\_NA - 49.11 * Fine\_WTC\ agg + 48.83 \\ & * Coarse\_WTC\ agg + 0.50 * W/C + 0.58 * SP \\ & + 11.65 \end{aligned} \quad (6)$$

Sulphate Resistance

Strength Loss:

$$\begin{aligned} Sulphate\ Strength\ Loss\ =\ & 1.90 * OPC - 1.90 * WCTPs - 1.71 \\ & * WBGNPs + 45.18 * Fine\_NA - 45.14 \\ & * Coarse\_NA - 45.18 * Fine\_WTC\ agg \\ & + 45.14 * Coarse\_WTC\ agg + 0.44 * W/C \\ & + 0.44 * SP + 7.79 \end{aligned} \quad (7)$$

Weight Loss:

$$\begin{aligned} Sulphate\ Weight\ Loss\ =\ & 0.14 * OPC - 0.14 * WCTPs - 0.23 \\ & * WBGNPs + 6.08 * Fine\_NA - 6.05 \\ & * Coarse\_NA - 6.08 * Fine\_WTC\ agg \\ & + 6.05 * Coarse\_WTC\ agg + 0.07 * W/C \\ & + 0.07 * SP + 2.38 \end{aligned} \quad (8)$$

Table 5
Performance metrics of the predictive model for four output parameters.

Output Parameter	R^2	MSE	MAE
Acid Strength Loss (12 months)	0.99	7.49	2.10
Acid Weight Loss (12 months)	0.97	0.41	0.54
Sulphate Strength Loss (12 months)	0.99	0.52	0.59
Sulphate Weight Loss (12 months)	0.98	0.01	0.08

4.3. Optimization of concrete mix design for minimizing strength and weight loss in acidic and sulphate environments

This study focuses on optimizing the concrete mix design to minimize both strength and weight loss when exposed to acidic and sulphate environments. The optimization process uses a SLSQP algorithm, solving a constrained optimization problem. The objective is to determine the ideal proportions of OPC, WCTPs, WBGNPs, aggregates, and SP to minimize concrete degradation over a 12-month period. Additionally, a constraint was introduced to ensure that the total weight of fine and coarse aggregates does not exceed 1700 kg/m^3.

The optimization problem is formulated as a multi-objective minimization task, where the goal is to minimize the following parameters:

- *Acid Strength Loss (12 months) (ASL12)*
- *Acid Weight Loss (12 months) (AWL12)*
- *Sulphate Strength Loss (12 months) (SSL12)*
- *Sulphate Weight Loss (12 months) (SWL12)*

The objective function *f(x)* to be minimized is:

$$f(x) = ASL12 + AWL12 + SSL12 + SWL12 \quad (9)$$

Constraints and Boundaries

The optimization is subject to the following constraints:

i. The input variables, including OPC, WTCPs, WBGNPs, and SP %, must stay within the ranges provided by the dataset.
ii. The total weight of fine and coarse aggregates must not exceed 1700 kg/m^3. This constraint can be mathematically expressed as:

Fine Aggregates + Coarse Aggregates $\leq$ 1700

Mathematically, the full set of constraints is defined as:

OPC min $\leq$ OPC $\leq$ OPC max

WTCPSs min $\leq$ WTCPs $\leq$ WTCPs max

WBGNPs min $\leq$ WBGNPs $\leq$ WBGNPs max

W/C min $\leq W/C \leq$ W/C max

SP % min $\leq$SP %$\leq$ SP % max

Fine Aggregates + Coarse Aggregates $\leq$ 1700

Optimization Algorithm: Sequential Least Squares Programming (SLSQP)

The SLSQP algorithm is applied to minimize the objective function while satisfying the constraints. SLSQP is a gradient-based optimization method that iterates through potential solutions by adjusting the input variables. The algorithm is designed to handle both equality and inequality constraints.

The optimization problem is mathematically expressed as:

$$min_x f(x) = ASL12 + AWL12 + SSL12 + SWL12 \quad (10)$$

subject to g(x)$\geq$0 and Fine Aggregates + Coarse Aggregates $\leq$1700

The flowchart for the optimization process is illustrated as follows:

Start → Define Objective Function → Define Input Variables and Constraints → Apply SLSQP Algorithm → Evaluate Total Loss → Iterate Until Convergence → Optimal Mix Design

The scatter plot shown in Fig. 21 illustrates the optimized concrete mix design parameters derived from the study aimed at minimizing strength and weight loss in acidic and sulphate environments. Each point represents a specific parameter, providing a clear visual overview

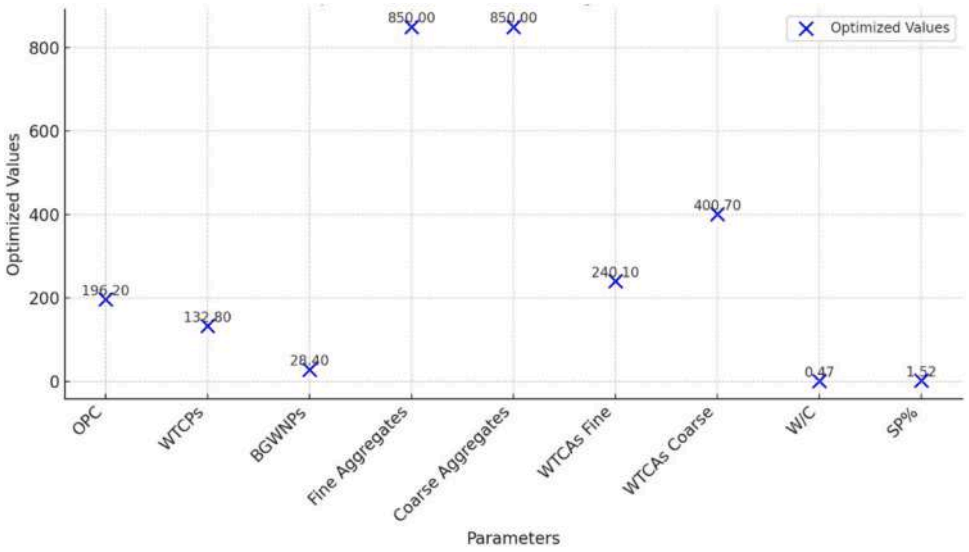

Fig. 21. Optimized concrete mix design parameters to minimizing strength and weight loss in acidic and sulphate environments.

of the optimized values. The data distribution highlights the balance between different components of the mix, showcasing how adjustments to the proportions can enhance concrete performance.

Future validation is planned to substantiate the SLSQP-optimized mix. The optimized mix and two dataset-bounded controls will be cast and evaluated for compressive strength (ASTM C39) and deterioration under acidic and sulphate exposure (ASTM C267, ASTM C1012) over 12 months. Outcomes (mass/strength loss and expansion at 1, 3, 6, 12 months; $n \geq 3$) will be analyzed by one-way ANOVA/Tukey, with validation indicated by significantly lower deterioration for the optimized mix.

5. Conclusions

This study demonstrated that replacing 60 % of OPC with WTCPs and incorporating 4–6 % WBGNPs significantly improved the durability of concrete exposed to acidic and sulfate environments. The improvements were attributed to enhanced microstructure, reduced gypsum and ettringite formation, and better resistance to degradation. AI-driven optimization further validated the mix design by minimizing strength and weight loss. The following results are concluded:

i. Modified concrete specimens were prepared by replacing 60 % of OPC with WTCPs at varying contents (2, 4, 6, 8, 10 %) of WBGNPs. Although replacing OPC with WTCPs and adding WBGNPs reduced workability, compressive strength improved significantly. At 28 days, compressive strength rose from 26.4 MPa in ceramic-based concrete to 36.9 MPa with 4 % WBGNPs, highlighting the densification of the cementitious matrix and enhanced durability under aggressive environments.
ii. The durability performance of the designed concrete was significantly enhanced with the inclusion WTCPs and WBGNPs in the cement matrix. The loss in strength of the proposed concrete when exposed to acid solution was sharply decreased with the inclusion of 60 % of WTCPs, 4 % of WBGNPs and 6 % of WBGNPs wherein the loss percent was reduced from 37.13 to 14.73 % after half year of exposure and from 74.26 to 37.96 % after one-year exposure in the acid solution, respectively.
iii. A similar trend (significant decrease) was observed for the weight loss, UPV readings and loss percentages with the inclusion the WTCPs and WBGNPs in the concrete mixes.
iv. From the visual appearance, it was found that the replacement of 60 % of OPC with WTCPs and incorporation of 6 % of WBGNPs could improve the specimens' resistance compared to other specimens, reducing the surface deterioration, number of cracks and their sizes.
v. The microstructures analysis of concrete via XRD, FESEM-EDX, and FTIR indicated a remarkable reduction in the calcium level in the cement matrix due to the replacement of OPC by WTCPs and BGWNPs, reducing the free Portlandite and expansive crystalline gypsum and ettringite formulation, leading to a decrease in the internal stress, expansion and micro-cracks of concrete.
vi. AI-driven analysis using a Random Forest Regressor achieved high predictive accuracy (R^2: 0.97–0.99) for strength and weight loss under acidic and sulfate environments. Sequential Least Squares Programming (SLSQP) optimized the mix design, incorporating 60 % WTCPs and 4–6 % WBGNPs, reducing sulfate strength loss to 1.45 % and weight loss to 0.41 % after 12 months, while ensuring aggregate content stayed below 1700 kg/m^3.
vii. The proposed concrete developed with high amount of wastes ceramic tiles and incorporated with silica nanoparticles can be highly recommended for the uses in aggressive environment such as sulphuric acid for it high resistance and excellent performance. Together, the proposed concrete can consider as eco-friendly construction materials for it benefits to reduce the landfill problems, re-use of the ceramic and glass wastes, reduce the demand of natural resources and contribute to low carbon footprint, thus meeting the sustainable development goals in 21st century.

CRediT authorship contribution statement

Zahraa Hussein Joudah: Writing – original draft, Resources, Methodology, Investigation, Formal analysis, Data curation. **Nur Hafizah A. Khalid:** Writing – review & editing, Validation, Supervision, Conceptualization. **Mohammad Hajmohammadian Baghban:** Writing – review & editing, Visualization, Validation, Supervision, Investigation, Funding acquisition, Conceptualization. **Iman Faridmehr:** Writing – review & editing, Visualization, Validation, Software, Project administration, Investigation, Formal analysis, Conceptualization. **Masoumeh Khamehchi:** Visualization, Validation, Software, Conceptualization. **Ghasan Fahim Huseien:** Writing – review & editing, Validation, Supervision, Investigation, Conceptualization.

Declaration of competing interest

The authors whose names are listed immediately below certify that

they have **NO** affiliations with or involvement in any organization or entity with any financial interest (such as honoraria; educational grants; participation in speakers' bureaus; membership, employment, consultancies, stock ownership, or other equity interest; and expert testimony or patent-licensing arrangements), or non-financial interest (such as personal or professional relationships, affiliations, knowledge or beliefs) in the subject matter or materials discussed in this manuscript. Author names:

Acknowledgments

The authors thank Universiti Teknologi Malaysia for their support and cooperation in conducting this research; grant number (R. J130000.7622.4C806 and Q.J130000.3822.22H88).

Data availability

Data will be made available on request.

References

[1] J. Xiao, et al., Experimental investigation on the influence of strength grade on the surface fractal dimension of concrete under sulfuric acid attack, Buildings 14 (3) (2024) 713.
[2] J. Xiao, et al., Influence of sulfuric acid corrosion on concrete stress–strain relationship under uniaxial compression, Measurement 187 (2022) 110318.
[3] S. Barbhuiya, D. Kumala, Behaviour of a sustainable concrete in acidic environment, Sustainability (2017).
[4] T.A. Abdalla, et al., Effect on sulfuric acid resistance and shrinkage of concrete incorporating processed bagasse ash and silica fume, Adv Civ Eng 2024 (1) (2024) 5534536.
[5] A.O.A.A.R. TANASH, K. Muthusamy, Concrete industry, environment issue, and green concrete: a review, Construction 2 (1) (2022) 01–09.
[6] A. Adesina, Recent advances in the concrete industry to reduce its carbon dioxide emissions, Environ. Chall. 1 (2020) 100004.
[7] M.Ö.A. Akan, D.G. Dhavale, J. Sarkis, Greenhouse gas emissions in the construction industry: an analysis and evaluation of a concrete supply chain, J. Clean. Prod. 167 (2017) 1195–1207.
[8] G.F. Huseien, et al., Optimizing mix design for alkali-activated concrete: a comprehensive review of critical selection factors, CivilEng 6 (3) (2025) 43.
[9] S.S. Altaher, et al., Optimizing mortar strength for infrastructure applications using rice husk ash and municipal solid waste incineration ash, Infrastructures 10 (10) (2025) 273.
[10] S. Gupta, H.W. Kua, C.Y. Low, Use of biochar as carbon sequestering additive in cement mortar, Cem. Concr. Compos. 87 (2018) 110–129.
[11] G.F. Huseien, et al., Sustainability of recycling waste ceramic tiles in the green concrete industry: a comprehensive review, Buildings 15 (14) (2025) 2406.
[12] A.M. Mhaya, et al., Long-term mechanical and durable properties of waste tires rubber crumbs replaced GBFS modified concretes, Constr. Build. Mater. 256 (2020) 119505.
[13] W. Shao, et al., Numerical modeling of chloride diffusion in cement-based materials considering calcium leaching and external sulfate attack, Constr. Build. Mater. 401 (2023) 132913.
[14] P.K. Mehta, Durability of concrete–fifty years of progress? Spec. Publ. 126 (1991) 1–32.
[15] R. Prakash, et al., An investigation of key mechanical and durability properties of coconut shell concrete with partial replacement of fly ash, Struct. Concr. 22 (2021) E985–E996.
[16] J. Yu, et al., Research on damage and deterioration of fiber concrete under acid rain environment based on GM (1, 1)-Markov, Materials 14 (21) (2021) 6326.
[17] S. Xie, L. Qi, D. Zhou, Investigation of the effects of acid rain on the deterioration of cement concrete using accelerated tests established in laboratory, Atmos. Env. 38 (27) (2004) 4457–4466.
[18] A. Arjomandi, et al., The effect of sulfuric acid attack on mechanical properties of steel fiber-reinforced concrete containing waste nylon aggregates: experiments and RSM-based optimization, J. Build. Eng. 64 (2023) 105500.
[19] J. Xiao, et al., Fractal characterization and mechanical behavior of pile–SOIL interface subjected to sulfuric acid, Fractals 29 (02) (2021) 2140010.
[20] J. Monteny, et al., Chemical and microbiological tests to simulate sulfuric acid corrosion of polymer-modified concrete, Cem. Concr. Res. 31 (9) (2001) 1359–1365.
[21] M. Mahmoud, M. Bassuoni, Response of concrete to incremental aggression of sulfuric acid, J. Test. Eval. 48 (4) (2020) 3220–3238.
[22] F. Girardi, R. Di Maggio, Resistance of concrete mixtures to cyclic sulfuric acid exposure and mixed sulfates: effect of the type of aggregate, Cem. Concr. Compos. 33 (2) (2011) 276–285.
[23] Y. Shen, et al., Influence of surface roughness and hydrophilicity on bonding strength of concrete-rock interface, Constr. Build. Mater. 213 (2019) 156–166.
[24] C. Shi, J. Stegemann, Acid corrosion resistance of different cementing materials, Cem. Concr. Res. 30 (5) (2000) 803–808.
[25] G.F. Huseien, et al., Durability performance of modified concrete incorporating fly ash and effective microorganism, Constr. Build. Mater. 267 (2021) 120947.
[26] M.M. Rashwan, A.R. Megahed, M.S. Essa, Effect of local metakaolin on properties of concrete and its sulphuric acid resistance, JES J. Eng. Sci. 43 (2) (2015) 183–199.
[27] J. Monteny, et al., Chemical, microbiological, and in situ test methods for biogenic sulfuric acid corrosion of concrete, Cem. Concr. Res. 30 (4) (2000) 623–634.
[28] S.T. Lee, et al., Effect of limestone filler on the deterioration of mortars and pastes exposed to sulfate solutions at ambient temperature, Cem. Concr. Res. 38 (1) (2008) 68–76.
[29] Djerfaf, N., Z. Nafa, and A.S. Eddine BELAIDI, Durability of high-performance concrete to an attack by a mixture of sulfuric acid and acetic acid. 2023. 75(1).
[30] M. Alexander, A. Bertron, N. De Belie, Performance of Cement-Based Materials in Aggressive Aqueous Environments, 10, Springer, 2013.
[31] S. Türkel, B. Felekoğlu, S. Dulluc, Influence of various acids on the physico-mechanical properties of pozzolanic cement mortars, Sadhana 32 (2007) 683–691.
[32] B. Osman, et al., Durability of concrete to sulfate attack under different environments, in: Advanced Materials and Structural Engineering: Proceedings of the International Conference On Advanced Materials and Engineering Structural Technology (ICAMEST 2015), April 25-26, 2015, CRC Press, Qingdao, China, 2016.
[33] V. Pavlík, Acid attack on hardened cement paste by acids forming low soluble calcium salts, in: IOP Conference Series: Materials Science and Engineering, IOP Publishing, 2019.
[34] E. Hewayde, et al., Using concrete admixtures for sulphuric acid resistance, Proc. Inst. Civ. Eng. Constr. Mater. 160 (1) (2007) 25–35.
[35] A. Chegenizadeh, et al., Sulphate attack on cemented-bentonite-coconut coir, Results Eng. 6 (2020) 100111.
[36] J. Xiao, et al., Three-dimensional fractal characterization of concrete surface subjected to sulfuric acid attacks, J. Nondestruct. Eval. 39 (2020) 1–15.
[37] C.M. Tibbetts, et al., Relating water permeability to electrical resistivity and chloride penetrability of concrete containing different supplementary cementitious materials, Cem. Concr. Compos. 107 (2020) 103491.
[38] M. Ariffin, et al., Sulfuric acid resistance of blended ash geopolymer concrete, Constr. Build. Mater. 43 (2013) 80–86.
[39] Z. Chen, H. Ye, Improving sulphuric acid resistance of slag-based binders by magnesium-modified activator and metakaolin substitution, Cem. Concr. Compos. 131 (2022) 104605.
[40] J. Xiao, et al., Study on the influence of three factors on mass loss and surface fractal dimension of concrete in sulfuric acid environments, Fractal Fract. 5 (4) (2021) 146.
[41] Z. Yu, et al., RETRACTED: Influence of Eco-Friendly Fine Aggregate On Macroscopic properties, Microstructure and Durability of Ultra-High Performance concrete: a Review, Elsevier, 2023.
[42] E.O. Nnadi, J. Lizarazo-Marriaga, Acid corrosion of plain and reinforced concrete sewage systems, J. Mater. Civ. Eng. 25 (9) (2013) 1353–1356.
[43] Z. Makhloufi, et al., Effect of mineral admixtures on resistance to sulfuric acid solution of mortars with quaternary binders, Phys. Procedia 55 (2014) 329–335.
[44] C. Cai, et al., Long-term shrinkage performance and anti-cracking technology of concrete under dry-cold environment with large temperature differences, Constr. Build. Mater. 349 (2022) 128730.
[45] I. Maruyama, et al., Effect of fineness of cement on drying shrinkage, Cem. Concr. Res. 161 (2022) 106961.
[46] P. Chindaprasirt, P. Sujumnongtokul, P. Posi, Durability and mechanical properties of pavement concrete containing bagasse ash, Mater. Today: Proc. 17 (2019) 1612–1626.
[47] E. Arif, M.W. Clark, N. Lake, Sugar cane bagasse ash from a high efficiency co-generation boiler: applications in cement and mortar production, Constr. Build. Mater. 128 (2016) 287–297.
[48] M.I. Khan, M.A.A. Sayyed, M.M.A. Ali, Examination of cement concrete containing micro silica and sugarcane bagasse ash subjected to sulphate and chloride attack, Mater. Today: Proc. 39 (2021) 558–562.
[49] K. Sothornchaiwit, et al., Influences of silica fume on compressive strength and chemical resistances of high calcium fly ash-based alkali-activated mortar, Sustainability 14 (5) (2022) 2652.
[50] A. Joshaghani, M.A. Moeini, Evaluating the effects of sugarcane-bagasse ash and rice-husk ash on the mechanical and durability properties of mortar, J. Mater. Civ. Eng. 30 (7) (2018) 04018144.
[51] G.H. Barbhuiya, et al., Effects of the nanosilica addition on cement concrete: a review, Mater. Today: Proc. 32 (2020) 560–566.
[52] L. Singh, et al., Beneficial role of nanosilica in cement based materials–A review, Constr. Build. Mater. 47 (2013) 1069–1077.
[53] P. Aggarwal, R.P. Singh, Y. Aggarwal, Use of nano-silica in cement based materials—A review, Cogent Eng. 2 (1) (2015) 1078018.
[54] M. Tabish, M.M. Zaheer, A. Baqi, Effect of nano-silica on mechanical, microstructural and durability properties of cement-based materials: a review, J. Build. Eng. 65 (2023) 105676.
[55] L. Varghese, V.V.L.K. Rao, L. Parameswaran, Nanosilica-added concrete: strength and its correlation with time-dependent properties, Proc. Inst. Civ. Eng. Constr. Mater. 172 (2) (2019) 85–94.
[56] P. Abhilash, et al., Effect of nano-silica in concrete; a review, Constr. Build. Mater. 278 (2021) 122347.
[57] G.F. Huseien, et al., Evaluation of high-volume fly-ash cementitious binders incorporating nanosilica as eco-friendly sustainable concrete repair materials, Constr. Build. Mater. 447 (2024) 138022.
[58] D.-C. Feng, et al., Machine learning-based compressive strength prediction for concrete: an adaptive boosting approach, Constr. Build. Mater. 230 (2020) 117000.

[59] M. Abdellatief, et al., A convolutional neural network-based deep learning approach for predicting surface chloride concentration of concrete in marine tidal zones, Sci. Rep. 15 (1) (2025) 27611.
[60] M. Sadagopan, K. Malaga, A. Nagy, Modified pycnometer method to measure the water absorption of crushed concrete aggregates, J. Sustain. Cem. Based Mater. 9 (5) (2020) 259–269.
[61] D. Zhang, R. Luo, Modifying the BET model for accurately determining specific surface area and surface energy components of aggregates, Constr. Build. Mater. 175 (2018) 653–663.
[62] G.W. Gee, D. Or, 2.4 Particle-size analysis. Methods soil anal: 4, Phys. methods 5 (2002) 255–293.
[63] H. Kabir, R.D. Hooton, N. Popoff, Evaluation of cement soundness using the ASTM C151 autoclave expansion test, Cem. Concr. Res. 136 (2020) 106159.
[64] P. Suraneni, et al., ASTM C618 fly ash specification: comparison with other specifications, shortcomings, and solutions, ACI Mater. J. 118 (1) (2021) 157167.
[65] Astm, C., Standard test method for sieve analysis of fine and coarse aggregates. ASTM C136-06, 2006.
[66] M.L. Kasulanati, R.K. Pancharathi, Gradation of aggregates using standard codes and particle packing methods-A comparative study, in: National Conference On Advances in Construction Materials and Management, Springer, 2022.
[67] Z.H. Joudah, et al., Development sustainable concrete with high-volume wastes tile ceramic: role of silica nanoparticles amalgamation, Case Stud. Constr. Mater. 21 (2024) e03733.
[68] A.M. Onaizi, et al., Effect of the addition of nano glass powder on the compressive strength of high volume fly ash modified concrete, Mater. Today: Proc. 48 (2022) 1789–1795.
[69] A.M. Onaizi, et al., Effect of nanomaterials inclusion on sustainability of cement-based concretes: a comprehensive review, Constr. Build. Mater. 306 (2021) 124850.
[70] M. Samadi, et al., Enhanced performance of nano-palm oil ash-based green mortar against sulphate environment, J. Build. Eng. 32 (2020) 101640.
[71] Z.F. Akbulut, et al., Exploring the flowability, physical, and mechanical properties of eco-friendly colored cement mortars with metakaolin under sulfuric (H2SO4) and nitric acid (HNO3) attacks, J Build Eng 91 (2024) 109463.
[72] B. Uzbas, A.C. Aydin, Microstructural analysis of silica fume concrete with scanning electron microscopy and X-ray diffraction, Eng. Technol. Appl. Sci. Res. 10 (3) (2020) 5845–5850.
[73] S.P. Yap, et al., Relationship between microstructure and performance of polypropylene fibre reinforced cement composites subjected to elevated temperature, Eur. J. Environ. Civ. Eng. 26 (5) (2022) 1792–1806.
[74] V.H.J.M. dos Santos, et al., Application of Fourier transform infrared spectroscopy (FTIR) coupled with multivariate regression for calcium carbonate (CaCO3) quantification in cement, Constr. Build. Mater. 313 (2021) 125413.
[75] P. Li, et al., Hydration and microstructure of cement paste mixed with seawater–An advanced investigation by sem-eds method, Constr. Build. Mater. 392 (2023) 131925.
[76] G.F. Huseien, et al., Alkali-activated mortars blended with glass bottle waste nano powder: environmental benefit and sustainability, J. Clean. Prod. 243 (2020) 118636.
[77] G.F. Huseien, A review on concrete composites modified with nanoparticles, J. Compos. Sci. 7 (2) (2023) 67.
[78] R.A. Elhefny, et al., Thermal degradation and microstructural evolution of geopolymer-based UHPC with silica fume and quartz powder, Infrastructures 10 (8) (2025) 192.
[79] M. Bassuoni, M. Nehdi, Resistance of self-consolidating concrete to sulfuric acid attack with consecutive pH reduction, Cem. Concr. Res. 37 (7) (2007) 1070–1084.
[80] V. Rodriguez-Galiano, et al., Machine learning predictive models for mineral prospectivity: an evaluation of neural networks, random forest, regression trees and support vector machines, Ore Geol. Rev. 71 (2015) 804–818.
[81] Y. Ma, N. Zhang, J. Li, Improved sequential least squares programming–driven feasible path algorithm for process optimisation. Computer Aided Chemical Engineering., Elsevier, 2022, pp. 1279–1284.